

PAULA DA FONSECA PEREIRA

**FUNCTIONAL CHARACTERIZATION OF THE MITOCHONDRIAL
ADENINE NUCLEOTIDE TRANSPORTER (ADNT1) IN *Arabidopsis thaliana*
UNDER DARK-INDUCED SENESCENCE**

Dissertation presented to the Universidade Federal de Viçosa as part of the requirements of the Pos-Graduate Program in Plant Physiology for obtention of the degree of *Magister Scientiae*.

**VICOSA
MINAS GERAIS - BRAZIL
2013**

PAULA DA FONSECA PEREIRA

**FUNCTIONAL CHARACTERIZATION OF THE MITOCHONDRIAL
ADENINE NUCLEOTIDE TRANSPORTER (ADNT1) IN *Arabidopsis thaliana*
UNDER DARK-INDUCED SENESCENCE**

Dissertation presented to the Universidade Federal de Viçosa as part of the requirements of the Pos-Graduate Program in Plant Physiology for obtention of the degree of *Magister Scientiae*.

APPROVED: FEBRUARY 28th, 2013

Wagner Luiz Araújo
(Co-advisor)

Marcelo Rogalski
(Co-advisor)

Dimas Mendes Ribeiro
(Member)

Adriano Nunes-Nesi
(Advisor)

Dedico esta dissertação às pessoas mais importantes da minha vida: meus pais e meus irmãos. Verdadeiros mestres, sempre acreditaram e me incentivaram a acreditar que eu era capaz de atingir meus objetivos.

AGRADECIMENTOS

Aos meus pais, Joaquim Rezende Pereira e Regina Célia da Fonseca Pereira, principais responsáveis pela minha vida e aos quais devo a enorme gratidão por terem me fornecido da forma mais amorosa os aprendizados necessários.

À minha irmã Vanessa pelo carinho e pelos constantes estímulos positivos para a realização deste trabalho. Valetinha, ter você como irmã é uma benção.

Ao meu irmão Guilherme por ter conseguido, através de suas demonstrações de admiração por mim, me motivar a ultrapassar as dificuldades.

Aos meus tios e tias, especialmente tio José Clério, tio Helvécio e Marina, tia Leninha, tia Lelé e tia Pité.

À Universidade Federal de Viçosa e ao Departamento de Biologia Vegetal que proporcionaram os meios para a realização do Curso de Mestrado.

À Fapemig pelo apoio financeiro.

Ao Professor Adriano Nunes-Nesi pelos direcionamentos, disposição e comprometimento em me orientar em benefício da solidificação dos meus alicerces profissionais.

Incluo, de forma especial, Alyne Lavinsky, Danielle Brito, Izabel Chaves, Jô França, Nayara e Renan Rocha. Agradeço a vocês pelo carinho, apoio e ajuda.

À Loba e à Lindinha pelo companheirismo.

Aos amigos: Alberto Abrantes, Auxiliadora Martins, Célia, Karina, David Medeiros, Fernanda Sartor, Franciele Oliveira, Fernanda Farnesi, Jéssica Terra, João Henrique, Jocimar Caiafa, Jorge Condoria, Luís Fernando, Franklin Magnum, Laíse Rosado, Lidiane Magalhães, Mariana Machado, Rebeca Omena, Renato Albernaz, Rinamara Rosa, Robson Loterio, Viviane Guzzo, Samira Alves e Eli pela amizade, pelo bom convívio, paciência e pelos momentos de descontração. A convivência com vocês é gratificante.

Aos Professores Wagner Araújo e Marcelo Rogalski pelos valiosos questionamentos e por terem sempre demonstrado muita receptividade e generosidade em esclarecer minhas dúvidas e em propor ideias que contribuísem positivamente para a realização dessa dissertação.

Aos Professores Raimundo, Marcelo Loureiro, Marcelo Rogalski e ao coordenador do programa, Fábio Murilo da Matta, por disponibilizarem a estrutura de seus laboratórios para a realização dos experimentos.

Aos funcionários Rogério Gomide, Carlos Raimundo, Geraldo, João Bosco, Oswaldo, Mercês, Antônio Cordeiro, Reginaldo, Luciene de Almeida, Sânzio Dias e Rosa pela ajuda e por tornarem as atividades na UFV menos monótonas.

Aos colegas de curso Priscila, Cris, Carlos Aucique, Regiane, Bruno, Medina, Marcela, Lorena, Genaína, Gil, Ana, Camila, Quida pelos momentos de estudo e descontração.

Aos colegas de laboratório: Paulo Silva, Rodrigo, Kelly Dettman, Leandro Elias, Samuel Cordeiro, Lucas Felisberto, Mariela, Lílian pela ajuda e convivência.

Aos demais professores do curso, funcionários e colegas, amigos distantes que, de alguma forma, auxiliaram na realização deste trabalho.

SUMÁRIO

| | |
|--|------|
| LISTA DE FIGURAS | vii |
| LISTA DE ABREVIACÕES..... | viii |
| RESUMO..... | x |
| ABSTRACT | xi |
| 1 INTRODUCTION | 1 |
| 2 MATERIAL AND METHODS..... | 8 |
| 2.1 Isolation and genetic characterization of an <i>Arabidopsis</i> mutant harboring a T-DNA insertion | 8 |
| 2.2 Dark treatment | 9 |
| 2.3 Processing and extraction | 9 |
| 2.4 Measurements of photosynthetic parameters | 10 |
| 2.5 Chlorophyll determination and measurement of photochemical efficiency..... | 10 |
| 2.6 Determination of sugars..... | 10 |
| 2.7 Determination of protein | 11 |
| 2.8 Determination of starch | 12 |
| 2.9 Determination of amino acids..... | 12 |
| 2.10 Determination of nitrate..... | 13 |
| 2.11 Determination of malate and fumarate | 14 |
| 2.12 Extraction, derivatization, and analysis of <i>Arabidopsis</i> leaf, metabolites by gas chromatography coupled to mass spectrometry | 14 |
| 2.13 Detemination of pyridine nucleotides..... | 15 |
| 2.14 Expression analysis by semiquantitative PCR..... | 16 |
| 2.15 Statistical analysis..... | 17 |
| 3 RESULTS | 17 |
| 3.1 Expression analysis by semiquantitative PCR..... | 17 |
| 3.2 Phenotypes of plants with lower expression of ADNT1 transporter..... | 17 |

| | |
|---|----|
| 3.3 Natural senescence phenotype in leaves of <i>Arabidopsis</i> genotypes with reduced expression of ADNT1 | 30 |
| 4 DISCUSSION..... | 32 |
| 4.1 Physiological relevance of ADNT1 in the metabolism of <i>Arabidopsis</i> | 32 |
| 5 REFERENCES | 36 |

LISTA DE FIGURAS

- Figure 1: Isolation and genetic characterization of an *Arabidopsis* ADNT1 18 mutant and antisense lines.
- Figure 2: Phenotypic characterization of *Arabidopsis* genotypes with 20 reduced expression of ADNT1 under extended dark treatment.
- Figure 3: Phenotype of *Arabidopsis* genotypes with reduced expression of 21 ADNT1 under extended dark treatment..
- Figure 4: Changes in the main carbon related compounds in leaves of 23 *Arabidopsis* genotypes with reduced expression of ADNT1 under extended dark treatment.
- Figure 5: Changes in the main nitrogen related compounds and organic acids 24 in leaves of *Arabidopsis* genotypes with reduced expression of ADNT1 under extended dark treatment.
- Figure 6: Relative levels of sugars and organic acids in leaves of 26 *Arabidopsis* genotypes with reduced expression of ADNT1 under extended dark treatment. as Measured by GC-MS.
- Figure 7 Relative levels of amino acids in leaves of *Arabidopsis* genotypes 27 with reduced expression of ADNT1 under extended dark treatment.
- Figure 8 Pyridine nucleotide levels and ratios in leaves of *Arabidopsis* 29 genotypes with reduced expression of ADNT1 under extended dark treatment.
- Figure 9 Effect of decreased ADNT1 expression on respiration and 30 photosynthetic parameters measurements performed in 4–5-week-old plants.
- Figure 10 Natural senescence phenotypes in leaves of *Arabidopsis* genotypes 31 with reduced expression of ADNT1.

LISTA DE ABREVIATURAS

| | |
|-------------------|---|
| AAC | ADP/ATP Carrier |
| ADH | Alcohol dehydrogenase |
| ADNT1 | Adenine nucleotide transporter 1 |
| ADP | Adenosine diphosphate |
| AOX | Alternative oxidase |
| AMP | Adenosine monophosphate |
| ATP | Adenosine triphosphate |
| BSA | Bovine serum albumin |
| Col-0 | Columbia0 |
| DC | Dicarboxylate carrier |
| DNA | Deoxyribonucleic acid |
| DTC | Dicarboxylate / tricarboxylate carrier |
| EDTA | Ethylenediamine tetraacetic acid |
| ETC | Electron transport chain |
| ETF-ETFQO | Flavoprotein:ubiquinone oxidoreductase |
| FAMEs | Fatty acid methyl esters |
| <i>Fm</i> | Maximal fluorescence |
| <i>Fv</i> | Variable fluorescence |
| FW | Fresh weight |
| GABA | Gamma-aminobutyric acid |
| GC-MS | Gas chromatography-mass spectrometry |
| G6PDH | Glucose 6-phosphate dehydrogenase |
| IRGA | Infrared gas analyser |
| KDa | Kilodalton |
| MCF | Mitochondrial Carrier Family |
| MSTFA | N-Methyl-N-(trimethylsilyl)trifluoroacetamide |
| MTT | Methylthiazolyldiphenyl-tetrazolium bromide |
| NAD ⁺ | Nicotinamide adenine dinucleotide |
| NADP ⁺ | Nicotinamide Adenine Dinucleotide Phosphate |
| NDT | Nicotinamide Adenine Dinucleotide Transporter |
| NR | Nitrate reductase |
| OD | Optical density |
| PCR | Polymerase Chain Reaction |
| PES | Phenazine ethosulfate |
| PMS | Phenazine methosulfate |
| PNC | Peroxisomal adenine nucleotide carrier |
| PSII | Photosystem II |
| Rd | Dark respiration |
| RNA | Ribonucleic acid |
| TCA | Tricarboxylic acid |
| T-DNA | Transfer DNA |
| UCP | Uncoupling protein |

WT *Wild type* (selvagem)
VDAC Voltage-dependent anion channels

RESUMO

PEREIRA, Paula da Fonseca, M. Sc., Universidade Federal de Viçosa, Fevereiro de 2013. **Caracterização functional do transportador mitochondrial de nucleotídeos de adenina (ADNT1) em plantas de *Arabidopsis thaliana* submetidas à condição de senescência induzida pela escuridão.** Orientador: Adriano Nunes Nesi. Coorientadores: Marcelo Rogalski e Wagner Luiz Araújo

Um novo transportador de nucleotídeos de adenina foi identificado na membrana mitocondrial interna de *Arabidopsis thaliana* e designado ADNT1 (At4g01100). Ao contrário de outros transportadores de ADP/ATP, ADNT1 é o único que medeia um antiporte um de ATP preferencialmente por AMP, e, em menor grau, por ADP. Um trabalho prévio sugere que a expressão ADNT1 é maior em pontas de raízes e em tecidos senescentes. Considerando a elevada expressão de ADNT1 em tecidos senescentes, nos propusemos a investigar o papel do ADNT1 durante o processo de senescência induzida pelo escuro. Sob estas condições, plantas mutantes de *Arabidopsis thaliana* deficientes na expressão do transportador ADNT1 exibiram uma senescência antecipada em relação ao tipo selvagem, como evidenciado tanto pelo fenótipo visual das plantas após o crescimento em longos períodos de escuridão, como pela perda de clorofilas e da capacidade fotossintética. O tratamento prolongado de escuro levou, em geral, a um declínio mais rápido nos mutantes do que nos do tipo selvagem nos teores de clorofila e nos níveis de sacarose e de proteínas. Por outro lado, os níveis de aminoácidos totais e de alguns intermediários do ciclo TCA, como malato, fumarato e isocitrato geralmente aumentaram significativamente nos mutantes no final do tratamento de escuro. As razões NADH/NAD⁺ e NADPH/NADP⁺ também se apresentaram maiores nos mutantes em comparação com o tipo selvagem, com a progressão da escuridão. Além disso, as plantas mutantes apresentaram sintomas de senescência precoce em comparação ao tipo selvagem, mesmo sob condições tidas como não estressantes. Estes dados demonstram, assim, que ADNT1 não é funcionalmente redundante aos previamente caracterizados transportadores de ADP/ATP, especialmente durante a falta de carbono, e reforçam a função potencial de ADNT1 no fornecimento da energia necessária para suportar o crescimento de tecidos vegetais heterotróficos.

ABSTRACT

PEREIRA, Paula da Fonseca, M. Sc., Universidade Federal de Viçosa, February, 2013.
Functional characterization of the mitochondrial adenine nucleotide transporter (ADNT1) in *Arabidopsis thaliana* under dark-induced senescence. Adviser: Adriano Nunes Nesi. Co-advisers: Marcelo Rogalski and Wagner Luiz Araújo

One novel adenine nucleotide transporter was identified in the inner mitochondrial membrane from *Arabidopsis thaliana* being designated as ADNT1 (At4g01100). Unlike other ADP/ATP carriers, ADNT1 is the only one that mediates an antiport of ATP, AMP, and, to a lesser extent, ADP and the corresponding deoxyadenine nucleotides. Previous work observed that ADNT1 expression is much stronger in root tips and senescent tissues. Considering the high expression of ADNT1 in senescent tissues, we have investigated the role of ADNT1 during the process of dark-induced senescence. Under these conditions, *Arabidopsis thaliana* mutants deficient in the expression of ADNT1 transporter displayed a similar, yet milder, early onset of senescence as evidenced both by the visual phenotype of plants following growth in extended periods of darkness and the loss of chlorophyll and photosynthetic competence. The extended dark treatment led in general to a more rapidly decline in the mutants than in the wild type in the levels of sucrose and protein. By contrast, the levels of total amino acids and TCA cycle intermediates malate, fumarate and isocitrate generally increased significantly in the mutants at the end of dark treatment. The NADH/NAD⁺ and NADPH/NADP⁺ ratios also increased in mutants in comparison to the wild type with progression of the darkness. Additionally, the mutant plants exhibited symptoms of early senescence in comparison to the wild type even under optimal conditions. Altogether the data obtained demonstrate that ADNT1 is not functionally redundant to the previously characterized ADP/ATP carriers, especially during carbon starvation and reinforce the potential function for ADNT1 in the provision of energy which is required to support growth in heterotrophic plant tissues.

1 INTRODUCTION

The vast majority of metabolic pathways within the highly compartmentalized plant cells are distributed across several cellular compartments, which in turn requires the activities of membrane transporters to catalyze the flux of precursors, intermediates, and end products between compartments. It is therefore not surprising that at least one and frequently more than one membrane separate organelles from the cytosol in eukaryotic cells (Brautigam & Weber, 2011). Accordingly such cell membranes are barriers necessary for the development of life by enabling single cells to support metabolic, reproductive, and developmental activities under stable physico-chemical conditions (Buchanan et al., 2000). Due to the hydrophobic nature of the lipid bilayer the sequestration of hydrophilic compounds, such as most of the nutrients and metabolites, allows the generation of different (bio)chemical environments within the cell (Poirier & Bucher, 2002).

Biological membranes allow cells to establish division and separation of biosynthetic functions and catabolic storage (Poirier & Bucher, 2002). This results in higher metabolic flexibility and efficiency by allowing the optimization of enzymatic reactions and, at the same time, supplying various subcellular pH environments. The plant cell compartmentalization also enables the simultaneous operation of several pathways that compete for the same substrates avoiding futile cycles and confining toxic byproducts in defined sub-cellular spaces (Linka & Weber, 2010).

Due to the hydrophobic nature of these membranes and coordinating the transport of various compounds across biological membranes, which is a prerequisite for the proper maintenance of metabolism (Mohlmann et al., 1998), specific transport proteins are required to facilitate and regulate the movement of metabolites across compartmental boundaries (Linka & Weber, 2010).

Most of the carriers in plants as well as in other eukaryotic organisms have not been identified at the molecular level yet (Tegeder and Weber, 2006; Lunn, 2007; Weber and Linka, 2011). Interestingly in *Arabidopsis thaliana* approximately 5% of the genome appears to encode membrane transport proteins (Maser *et al.*, 2001). It should be mentioned, however, that even considering the importance of these transporters to the proper functioning of plant metabolism, our current knowledge about them remains rather fragmented. This situation is even more complicated in the specific case of mitochondrial transporters where, for example, many transport processes have not yet been properly described. There is a clear need to transport metabolites, cofactors and nucleotides into and out of mitochondria in order to precisely connect the various metabolic processes (Picaut *et al.*, 2004). Thus within the outer mitochondrial membrane, the transport is largely accomplished by voltage-dependent anion channels (VDAC) or porins which form pores allowing the movement of solutes with more than 1,000 Da (Millar *et al.*, 2011; Duncan *et al.*, 2013). By contrast, the inner mitochondrial membrane is generally impermeable to charged or polar molecules. This is mainly due to the ATP synthesis via oxidative phosphorylation in mitochondria which depends on the electrochemical gradient of protons across this membrane (Picaut *et al.*, 2004). Accordingly, import and export of metabolites across mitochondrial membranes are processes highly regulated and controlled at the level of the inner mitochondrial membrane (Nury *et al.*, 2006). Therefore, as opposed to the outer membrane, only small molecules or uncharged gases such as oxygen and carbon dioxide can readily cross the inner mitochondrial membrane (Palmieri *et al.*, 2011).

Nuclear encoded proteins of the mitochondrial carrier family (MCF), which are located mainly in the inner mitochondrial membrane, mediate the transport of a large range of metabolic intermediates (Palmieri *et al.*, 2011). Whilst the members of the

MCF are highly heterogeneous in terms of substrate specificity and mode of transport, all members have a similar molecular weight (30-35 kDa) and consist of six membrane spanning helices, exhibiting typical conserved domains and appearing as homodimers in the native membrane (Palmieri et al., 2011; Haferkamp & Schmitz-Esser, 2012). The primary structure of MCF members consists of three homologous domains repeated in tandem, with about 100 amino acids (Saraste & Walker, 1982). Each domain contains two hydrophobic segments (spanning the membrane as α -helices) and a characteristic amino acid sequence motif (Palmieri et al., 2011). Although structurally related (as discussed above), MCF proteins catalyze the specific transport of various substrates, such as nucleotides, amino acids, dicarboxylates, cofactors, phosphate or H^+ (Haferkamp & Schmitz-Esser, 2012). It has been recently demonstrated that MCF members also occurs in various other cell compartments and therefore their location and physiological function is not restricted to mitochondria only (Palmieri et al., 2011). In addition to MCF carrier proteins, other organelles contain a variety of carriers belonging to different families that apparently originated due to different events (Haferkamp & Schmitz-Esser, 2012). Intriguingly the relevance of MCF is further reinforced by the fact that MCF proteins are the only solute carriers present in the inner mitochondrial membrane (Haferkamp & Schmitz-Esser, 2012).

The combination of overexpression and transport studies in liposomes coupled with proteomics investigations of mitochondrial membranes obtained from genetically modified plants have identified several specific MCF such as AAC (ADP/ATP Carrier) (Haferkamp et al., 2002), dicarboxylate/tricarboxylate carrier (DTC) (Picaut et al., 2002), Dicarboxylate Carrier (DC) (Palmieri et al., 2007), NDT (Nicotinamide Adenine Dinucleotide Transporter) (Palmieri et al., 2009) amongst others. It is important to mention however that our current understanding of metabolite transport is still

hampered mainly due to the fact that there is still an increasing identification and characterization of carrier proteins (Picault et al., 2002; Millar and Heazlewood, 2003; Palmieri et al., 2009; Castegna et al., 2010; Eisenhut et al 2012).

It is well known that MCF members transport important compounds (Millar et al., 2011), among which are the nucleotides. Nucleotides are the main source of energy for living organisms playing a critical role in the synthesis of both DNA and RNA (Reinhold et al., 2007). Being not only required for the accumulation of polysaccharides nucleotides also serve as essential cofactors for a variety of enzymes (Reinhold et al., 2007), and participate in both intra and extra cellular signalling (Jeter et al., 2004, Reinhold et al. 2007). In particular, adenine nucleotides play a key role in plant energy metabolism and physiology (Haferkamp et al., 2011). Accordingly adenine nucleotide occurs at relatively high concentrations in all cells to support a wide range of functions (Klingenberg, 2008). Given this wide distribution and because of the important role of mitochondria in energy production it is tempting to suggest that the first MCF protein was also involved in energy passage (ADP/ATP exchange) (Haferkamp & Schmitz-Esser, 2012). Notwithstanding this transport across biomembranes demands a carrier with highly efficient catalytic qualities (Klingenberg, 2008), most likely due to the characteristics of adenine nucleotides such as molecular structure and large highly loaded.

In *higher* plants several adenine nucleotides carriers have been identified at the molecular level (Lerch et al., 2008; Linka et al., 2008, Geienberger et al., 2010, Yin et al. 2010, Rieder and Neuhaus, 2011). The plastidial ADP / ATP carrier promotes the absorption of ATP by both chloroplasts and heterotrophic plastids to allow the nocturnal ATP supply required for normal chlorophyll biosynthesis (Reiser et al., 2004; Reinhold et al., 2007; Linka et al., 2008). Likewise, in plastids of heterotrophic organs ATP

absorption occurs to drive biosynthesis of starch (Linka et al., 2008). In addition, at the endoplasmic reticulum membrane there is also an ADP/ATP antiport which enables ATP import to make possible the accumulation of proteins and lipids associated to the endoplasmic reticulum function (Lerch et al., 2008).

Two adenine nucleotides transport proteins have been recently identified in peroxisomes (PNC1 and PNC2) of *Arabidopsis* (Linka et al., 2008). Complementation in yeast and *in vitro* absorption assays showed that both protein catalyze the counter exchange of ATP with ADP or AMP (Linka et al., 2008). The import of ATP performed by both PNC1 and PNC2 is essential for the activation of fatty acids during germination and has also an additional role in other reactions of beta oxidation in peroxisomes, such as auxin metabolism (Linka et al., 2008).

Among MCF members, the ADP/ATP carrier (AAC) is the most abundant transporter found in the inner mitochondrial membrane (Haferkamp et al., 2011; Nury et al., 2006; Lerch et al., 2008) and, alongside the phosphate carrier seems to be essential for proper mitochondrial metabolism (Nury et al., 2006). ATP is the universal currency of energy for all living cells (Reiser et al., 2004). Being involved in most of the biochemical pathways in the cells it is not surprisingly that ATP carrier proteins play an indispensable role in coupling endergonic and exergonic reactions (Geigenberger et al., 2010). Thus, the passage of ADP / ATP mediated by these carriers through the inner mitochondrial membrane is likely to play a metabolic central role and is therefore a critical step in the supply of ATP from mitochondria into the cytosol (Klingenberg, 2008).

The AAC was the first member of the MCF to be characterized into details (Haferkamp et al., 2002). Thus, many of the findings about the structure and mechanism of mitochondrial transporters were first produced by studies with this carrier (Nury et al.

2006). Typical AAC proteins reside in mitochondria and catalyze the exchange of internal ATP to external ADP in a 1:1 rate and therefore supply the cytosol, mitochondria and other organelles with energy (Haferkamp et al., 2011). These carriers are structurally and functionally highly related to their orthologs from animals and yeast and exhibit identical substrate specificities. Moreover their transport characteristics are similarly influenced by the membrane potential (Haferkamp et al., 2002). Although three confirmed AAC isoforms (AAC1–3) are encoded in the *Arabidopsis* genome, evidence has demonstrated that it contains up to seven highly orthologous sequences (AAC-like genes) (Palmieri et al., 2011). Recent proteomic analyzes have suggested that isoforms of AAC proteins have an important role in housekeeping functions and, at least in the case of AAC2, direct involvement in adaptive responses to stress (Taylor et al., 2010). It has been also pointed out a potentially important role for the ACCs in programmed cell death (Swidzinski et al., 2002). Altogether these results clearly demonstrated that the function of ACC and by extension the MCF members are intimately associated with the mitochondrial function itself.

Despite the previously characterized AAC proteins (Haferkamp et al., 2002), another adenine nucleotide transporter, At4g01100 gene product, was recently identified in the inner mitochondrial membrane from *Arabidopsis thaliana* being designated as ADNT1 (At4g01100) (Palmieri et al., 2008). Localization experiments using GFP (green fluorescent protein) fusion demonstrated that the protein is exclusively directed to mitochondria (Palmieri et al. 2008). Furthermore, it was demonstrated tissue-constitutive expression of ADNT1, although staining of promoter-GUS fusions suggested that the expression was much stronger in root tips and senescing tissues (Palmieri et al., 2008). It is important to note, however, that ADNT1 function differs markedly from the ADP/ATP carriers characterized in yeast, human and *Arabidopsis* to

date. This is most likely due to the fact that ADNT1 mediates an antiport of ATP, AMP and, to a lesser extent, ADP and their corresponding deoxynucleotides nucleotides and is not inhibited by either bongrekate or carboxyatractyloside, inhibitors of the previously characterized AAC carriers (Palmieri et al., 2008).

It is reasonable to assume that ADNT1 could play a key role in oxidative phosphorylation, an assumption further supported by the fact that plants with T-DNA insertion in the gene At4g01100 exhibit a largely unaltered photosynthetic phenotype, but lower root respiration and growth compared to its wild type counterpart (Palmieri et al., 2008). Additionally, the identification of ADNT1 provides a molecular entity capable of exporting ATP (in exchange for cytosolic AMP) from the mitochondria to the cytosol in amounts sufficient to allow both the phosphorylation of AMP mediated by the adenylate kinase and the conversion of this nucleotide to ATP (Palmieri et al. 2008). Considering the essential role of ATP during mitochondrial respiration it is plausible to suggest a strict association between this important metabolic process and ADNT1. However, this is perhaps not surprising given the size and substrate diversity of the MCF (Palmieri et al., 2011) alongside the physiological evidence of rapid metabolite exchange across mitochondrial membranes (Hanning & Heldt, 1993).

In addition to alternative electron donors to ETCs, plant respiration is distinguished by the presence of plant-specific nucleotide transporters as discussed above. With that in mind, the preference of ADNT1 for AMP coupled with its high expression in root tips and senescent tissue allow us to speculate an important alternative role for the ADNT1 carriers. Taken together, these information highlight a current need for more detailed studies about ADNT1 in order to characterize to what extent it is important to sustain respiration in plant tissues, especially under conditions of carbon starvation. Thus the main goal of this work was to obtain a clear picture of the

functional role of the ADNT1 following growth in extended dark periods. The results obtained are discussed both in the context of the function of mitochondrial ATP transport in general and with respect to current models of metabolic shifts occurring during dark-induced senescence.

2 MATERIAL AND METHODS

The experiments were performed in Viçosa (20°45'S, 650 m altitude), Minas Gerais, at the Universidade Federal de Viçosa. I used wild plants (WT) and transgenic *Arabidopsis thaliana* plants, ecotype Col-0 kindly provided by Dr. Alisdair R. Fernie, at the Max Planck Institute for Molecular Plant Physiology, Golm-Potsdam, Germany.

2.1 Isolation and genetic characterization of an *Arabidopsis* mutant harboring a T-DNA insertion within ADNT1

As a first analysis of the *in vivo* role of the *Arabidopsis* ADNT1 protein, a PCR-based strategy was used to screen the GABI-Kat mutant population of T-DNA-tagged *Arabidopsis* plants (Rosso et al., 2003) for disruption of the ADNT1 gene (Palmieri et al., 2008). The 451B06 GABI-Kat line, carrying a T-DNA insertion in the ADNT1 gene, has been previously characterized (Palmieri et al., 2008). This line carries a single T-DNA insertion within the first intron of the ADNT1 gene (Figure 1A) and was obtained by *Agrobacterium*-mediated transformation according to the floral dip method (Clough and Bent, 1998). This line presents a resistance marker gene *su/I* to the antibiotic sulfadiazine.

In addition to the knockout mutant of ADNT1, antisense plants were created by expressing the complete ADNT1 coding sequence in the opposite orientation in the Gateway pK2WG7 vector (Palmieri et al., 2008) (Figure 1B). Transgenic lines were

selected on kanamycin and screened at the expression level. Antisense lines displayed decreases in expression to 42% (line 10) and 35% (line 22) of wild-type levels (Palmieri et al., 2008).

2.2 Dark treatment

For dark treatments, 7- to 10-d-old seedlings were transferred to soil and then grown at 22°C under short-day conditions (8 h light/16 h dark) for 4 weeks. Following bolting, plants were grown at 22°C in the dark in the same growth cabinet. Four leaves per plant were harvested at intervals of 0, 3, 7, 10, and 15 days from control and dark-grown plants for subsequent analysis. Due to the limited amount of leaf material per plant, a composite sample of three plants was made.

2.3 Processing and extraction

The samples contained in tubes of 1.5 ml were pulverized in liquid nitrogen and subsequently metabolites were extracted in ethanol as Gibon et al. (2004) and Nunes-Nesi et al. (2005 and 2007). For leaf samples 250 µL of 98% ethanol were added in each tube, followed by homogenization, shaking and incubation for 20 min at 80°C. Then the samples were centrifuged for 5 minutes at 13,000 rpm at 4°C. Subsequently, the supernatant was collected in a new tube and the precipitate subjected to two further extractions with 150 µL and 250 µL of ethanol 80% and 50%, respectively. The ethanol extracts were combined in a single tube for subsequent quantification of metabolites. The precipitate was washed twice in 80% ethanol and stored at -20°C for later quantification of starch and protein according to Gibon et al. (2004).

2.4 Measurements of photosynthetic parameters

Gas exchange and chlorophyll fluorescence analysis were made on fully expanded four weeks leaves of *Arabidopsis thaliana*. For that end an infrared gas analyzer coupled fluorometer (IRGA, Li-cor Li-6400XT Inc., Lincoln, USA) was used for determining the rate of liquid carbon assimilation (A, $\text{CO}_2 \mu\text{mol m}^{-2} \text{s}^{-1}$), stomatal conductance (gs, $\text{mol H}_2\text{O m}^{-2} \text{s}^{-1}$) and internal CO_2 concentration (Ci , $\mu\text{mol CO}_2 \text{mol}^{-1}$). The estimation of these parameters relating the fluorescence proceeded as described by Lima et al. (2002).

2.5 Chlorophyll determination and measurement of photochemical efficiency

Chlorophyll content was determined as described in the literature (Porra et al., 1989). By using a microplate reader (OptiMax Tunable Microplate Reader, absorbance readings were taken of each sample at 645 and 665 nm. Once obtained the absorbances were calculated concentrations of chlorophyll *a* and *b* by the equations A and B, and the total content normalized by fresh weight of the sample.

$$\text{Chlorophyll } a = 5,21 * \text{Abs}_{665} - 2,07 * \text{Abs}_{645} \quad (\text{A})$$

$$\text{Chlorophyll } b = 9,29 * \text{Abs}_{645} - 2,74 * \text{Abs}_{665} \quad (\text{B})$$

The ratio of *Fv* to *Fm*, which corresponds to the potential quantum yield of the photochemical reactions of PSII, was measured as previously described (Oh et al., 1996) as a measure of the photochemical efficiency.

2.6 Determination of sugars

The levels of glucose, fructose and sucrose were determined in the soluble fraction ethanol as previously described (Fernie et al., 2001). For a 96-well microplate

was prepared a mixture containing 15.5 ml of buffer (HEPES/KOH 1 M, MgCl₂ 30 mM (pH 7,0) 0.1 X 480 µL of ATP [60mg/mL] 480 µL of NADP [36mg/mL] and 80 µL of glucose-6-phosphate dehydrogenase (G6PDH) [5 mg / mL]. Once prepared the mixture, 160 µL of the same was added to each well of microplate, to which were added 60 µL of ethanol extract. In the same microplate reader described above, absorbance readings were made of the respective samples at 340 nm in one minute intervals. Once stabilized the optical density (OD), were successively added 10 µL of hexokinase [1.5 U / well], 10 µL of phosphoglucose isomerase [1.5 U / well] and 10 µL of invertase [5U/ well]. To calculate the concentration of the respective sugars was used the equation C.

$$\mu\text{mol NADPH} = \Delta\text{OD}/(2,85*6,22) \quad (\text{C})$$

2.7 Determination of protein

Protein content was determined as in Gibon et al. (2004). To the tubes containing the precipitate, corresponding to fraction insoluble in ethanol, 400 µL of NaOH 0.1 M were added. After resuspending the precipitate, the samples were incubated for 1 h at 95°C under 500 g of agitation. Subsequently, the tubes were centrifuged at 13,000 rpm for 5 minutes. Subsequently were removed 3 µL of supernatant which was added to a microplate containing in each well 180 µL of Bradford reagent 1/5. On the same microplate reader, the absorbance was determined at a wavelength of 595 nm. The content of protein of each sample was determined using a standard curve of bovine serum albumin (BSA) made with the following concentrations: 0, 0.08, 0.16, 0.24, 0.32, 0, 40, 0.60, 0.80 mg / µL protein. The protein content was normalized by the fresh weight of the samples.

2.8 Determination of starch

Starch content was measured as previously described (Fernie et al., 2001). To the tubes containing the precipitate suspended in 0.1 M NaOH used in the determination of protein, was added 70 μ L of of 1M acetic acid for neutralization of the extract. The tubes were then agitated with the aid of a shaker tube and then 40 μ L of suspension were collected and placed in each well of the microplate. For starch degradation, a mix was prepared containing the enzymes amyloglucosidase and α -amylase resuspended in 0.5 M of sodium acetate pH 4.9 (proportion that for every 25 ml of 0.5 M sodium acetate pH 4.9, uses 500 μ L of amyloglucosidase and 5 μ L of of α -amylase). From this mix, withdrew 60 μ L, which was added to 40 μ L of suspension previously added to the wells of the microplate. Then the plate was sealed with aluminum tape (3M Model 425[®] HD) resistant to high temperature and incubated for one hour at 55 °C. After this step, the plates were centrifuged for 10 seconds at 10,000 g and then 50 μ L of the suspension was transferred to a new plate where were added to each well 160 μ L of a mixture containing 15.5 ml of HEPES / KOH buffer 1M, pH 7.0, 30 mM MgCl₂, 480 μ L of ATP [60mg/mL] 480 μ L of NADP [36mg/mL] and 80 μ L of glucose-6-phosphate dehydrogenase (0.7 U / μ L). By using an microplate reader, mentioned earlier, the absorbances were read at 340 nm in one minute intervals. Once stabilized the OD was added 10 μ L of hexokinase [2U/well]. To calculate the concentration of glucose and in turn the content of starch was used the equation C. The values were normalized by the fresh weight of the samples.

2.9 Determination of amino acids

Total amino acids were determined as by Gibon et al. (2004). In one microplate 50 μ L of 1 M citrate buffer, pH 5.2 with ascorbic acid 0.2% (w / v), 50 μ L of ethanol

extract and 100 mL of ninhydrin solution of 1% (w / v in 70% ethanol) were added to each well. Then the plate was sealed with an aluminum tape, resistant to high temperature (3M Model 425[®] HD) and incubated for 20 min at 95 ° C. After incubation, the plates were centrifuged for 10 sec at 10,000 rpm and subsequently the samples were transferred to a new microplate and readings were made at 570 nm.

For the determination of total amino acid content in the samples, a standard curve of Leucine was performed with the following concentrations: 0, 0.01, 0.025, 0.05, 0.1 and 0.25 mM. Once estimated amino acid concentrations in each well, the values were normalized by fresh weight of the sample.

2.10 Determination of nitrate

Nitrate content was determined following the protocol described by Fritz et al., (2006). In one microplate (P1) 10 µL of buffer consisting of 1M phosphate buffer, pH 7.5 and 0.5 µL of the NADPH 50 mM prepared in 5 mM NaOH, 10 µL of nitrate reductase [0.005 U / well prepared in 0.1 M phosphate buffer], 69.5 µL of H₂O and 10 µL of ethanol extract diluted 20 times in 80% ethanol were added to each well. In order to discount the nitrite content already present in the sample and quantify only the content of nitrite derived from nitrate reduction, another micowell plate (P2) was mounted, in which NR enzyme was not added to the aliquot being replaced by 10 µL of water. Once assembled the two plates, they were incubated in the dark for 30 min at 25 ° C. 15 µL of fenazinametosulfato 0.25 mM were added to each well of the respective plates, and then incubated again for 20 min at 25 ° C. Thereafter was added 60 µL of sulfanilamide 1% (w/v in 3M phosphoric acid) and 60 µL of N-(1-naphthyl)-ethylenediamine 0.02 % w / v. Finally, both plates were incubated for 10 min at 25 ° C and then read in a microplate reader at 540 nm. To determine only the nitrate content in

the samples, the absorbance value of each sample of the microplate P1 has been subtracted from the absorbance of microplate P2.

For the determination of total nitrate content in the samples, I performed a calibration curve of nitrate KNO_3 in the following concentrations: 0, 0.4, 0.8 and 1.6 mM. Once calculated nitrate concentrations in the wells, the values were normalized by fresh weight of the sample.

2.11 Malate and fumarate content

Malate and fumarate content were determined as in Nunes-Nesi et al. (2007). In one microplate 25 μL of buffer (Tricine / KOH 0.4 M, pH 9), 10 μL of MTT (methylthiazolyldiphenyl-tetrazolium bromide) 10 mM, 5 μL of NAD^+ [60 mM], 2 μL of fenazinaetosulfato [20 mM], 10 μL of Triton X100 10% (v / v), 33 μL of H_2O and 10 μL of ethanol extract were added to each well. Then, using a microplate reader, mentioned earlier, the absorbances were read at 570 nm at one minute intervals. Once stabilized OD, I successively added 10 μL of malate dehydrogenase [1,000 U / mL in 0.4 M tricine buffer, pH 9.0], and 10 μL of fumarase [100 U/ml 0.4 M tricine buffer, pH 9]. To calculate the concentration of malate and fumarate in the samples a standard curve prepared from malic acid and fumaric acid at the following concentrations: 0, 150, 300, 450, 600, 800, 1000 mM was used. Once calculated concentrations of malate and fumarate in the wells, the values were normalized by the fresh weight of the sample.

2.12 Extraction, derivatization, and analysis of *Arabidopsis* leaf, metabolites by gas chromatography coupled to mass spectrometry

Leaf samples collected were quickly frozen in liquid nitrogen and stored at -80°C until further use. For the determination of metabolites such as amino acids,

organic acids, sugars, among others, the procedure described by Lisec et al. (2006) was adopted. Around 25 mg of leaf powder were aliquoted into 1.5 ml tube and 1.5 mL of pre-chilled extraction solvent mixture (water, methanol and chloroform mixed in volumes in proportion 1: 2,5: 1) and 60 µL of ribitol (stock 0,2mg/mL) was added to each tube. Samples were vortex for about 10 sec, shaken for 30 min at 4°C in a thermomixer at 1000 rpm and centrifuged for 5 minutes at 13.000 rpm at 4°C. The supernatant was transferred to a new tube where it was added 750 µL of ultrapure water. The samples were vortex for 10 sec and centrifuged again for 15 min at 13.000 rpm at 4°C. The top layer (polar phase) was collected. Aliquots of 200 µL from each sample were taken. The samples were dried in a vacuum container and stored at -80°C until further use. For derivatization, it was added 40 µl of methoxyamination reagent to each sample and shaken at 37 °C for 2 h. 70 µl of N-Methyl-N-(trimethylsilyl)trifluoroacetamide (MSTFA) reagent and time standards fatty acid methyl esters (FAMEs) were added to samples, and shaken at 37 °C for 30 min. Aliquots were transferred to glass vials and analyzed by gas chromatography-mass spectrometry (GC-MS). For these analyzes was used GC-MS system according to Roessner et al. (2001) and Lisec et al. (2006). Identification and annotation concerning the metabolites followed recent recommendations for metabolic profiling (Fernie et al., 2011).

2.13 Pyridine nucleotides

NAD(H) and NADP(H) were determined as described by Schippers et al. (2008). Around 25 mg of leaf powder were aliquoted twice into 1.5 ml tube. NAD⁺ and NADP⁺ were extracted with 250 µl of 0.1 M HClO₄ and NADH⁺ and NADPH were extract with 250 µl 0.1 M KOH. Reduced and oxidized forms are distinguished by

preferential destruction in acid or base, respectively. The powder was immediately suspended after adding the solution by tapping and vortex. The samples were incubate 10 min on ice and centrifuged at 14 000 rpm for 10 min at 4°C. 200 µl of supernatant were taken into a new tube that was boiled for 2 min, rapidly cooled on ice, and neutralized as follows. All the following steps were done on ice. The alkaline extract was neutralized by adding 200 µl of 0.1 M HClO₄ in 0.2 M Tris pH 8.4 and the acid extract was neutralized with 200 µl of 0.1 M KOH in 0.2 M Tris pH 8.4. The final pH of the neutralized extracts was between 8.0 and 8.5. The pH of the samples were checked with pH test paper. NADP(H) were measured in the presence of 9 U·mL⁻¹ of glucose-6-phosphate dehydrogenase (G6PDH) grade I, 0.3M Tricine/KOH, pH 9.0, 12 mM Na₂-EDTA, 0.3 M of phenazine methosulfate (PMS), 1.8 mM methylthiazolyldiphenyl-tetrazolium bromide (MTT), and 9 mM glucose-6-phosphate. NAD(H) was measured in the presence of 18 U·mL⁻¹ alcohol dehydrogenase (ADH), 0.3M Tricine/KOH, pH 9.0, 12 mM Na₂-EDTA, 0.3 mM phenazine ethosulfate (PES), 1.8 mM MTT, and 1,5 M ethanol. The absorbance was followed at 570 nm at 30°C until the rates were stabilized. The rates of reactions were calculated as the increase of the absorbance in mOD min⁻¹.

2.14 Expression analysis by semiquantitative PCR

This analysis was performed with 4- week- old plants. For Total RNA was isolated and purified using TRIzol® Reagent (Life Technologies) according to the manufacturer's protocol. Three micrograms of RNA were used as template for first-strand cDNA synthesis using ImProm-II™Reverse Transcriptase System and an oligo (dT) primer. Primer pairs for Real-Time PCR were designed using the open-source program *QuantPrime-qPCR primer designed tool* (Arvidsson et al., 2008) (Table 1).

PCR program was 2 min at 94°C and 40× cycles (94°C for 30 sec/58°C for 30 sec/72°C for 1 minute). Separation of real-time PCR products on 2% (w/v) agarose gels revealed single bands of the expected size.

The gene-specific oligonucleotides used for PCR were: Adenine nucleotide transporter1 (ADNT1) forward 5'-TGGAAAGGCTAACTGTCCAGACC-3', reverse 5'-TGGAAGCCAACCACGGTACAAG-3'; Glyceraldehyde-3-phosphate dehydrogenase (GAPDH) forward 5'-TGGTTGATCTCGTTGTGCAGGTCTC-3', reverse 5'-GTCAGCCAAGTCAACAACTCTCTG -3'.

2.15 Statistical analysis

Where two observations are described in the text as different, this means that they were determined to be statistically different ($P < 0.05$) by the performance of Student's *t* test. All analysis were performed by a completely randomized design.

3 RESULTS

3.1 Expression analysis by semiquantitative PCR

To confirm the degree of repression of ADNT1 mRNA in the transgenic lines previously characterized by Palmieri et al (2008), we assessed ADNT1 steady state transcript levels using semiquantitative PCR (Figure 1C). For that aim cDNA of 4-week old plants from all genotypes analyzed here were used. As it can be seen, in comparison to WT levels the knockout mutant *adnt1* displayed clear reduction in the expression of ADNT1, while the antisense lines displayed minor decreases in expression of ADNT1, with a greater reduction in the line 10.

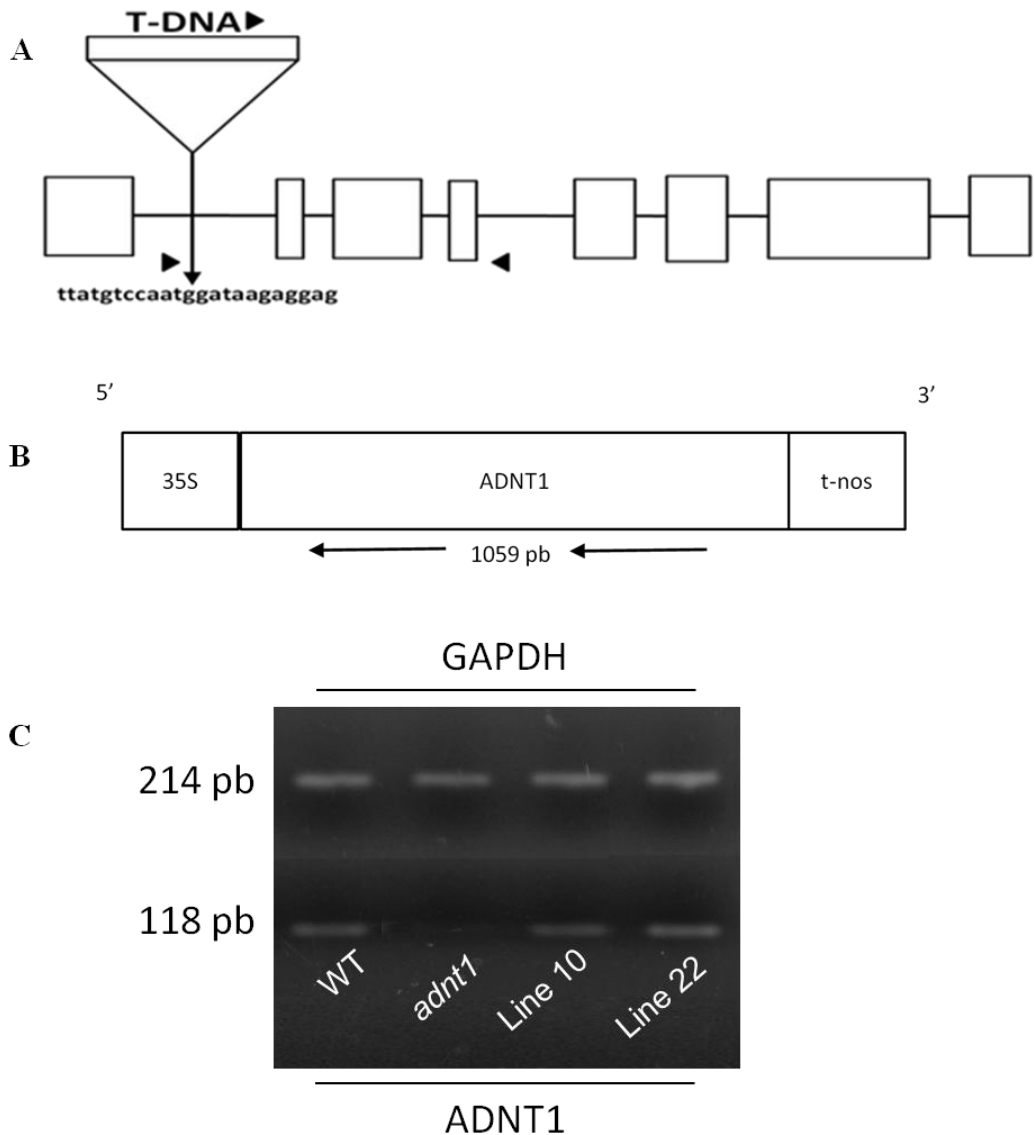


Figure 1. Isolation and genetic characterization of an *Arabidopsis* ADNT1 mutant and antisense lines. (A) Schematic representation of the ADNT1 gene. The mutant obtained by PCR screening of a T-DNA mutant collection (GABI-Kat) carries an insertion into the first intron of ADNT1. The scale of the T-DNA (approximately 4.5 kb) was not preserved for the sake of convenience. Boxes represent gene exons, and arrows on T-DNA, intron I, and intron IV denote primer positions for T2 and T3 population screening. (B) Schematic representation of antisense construct. (C) Expression analysis of ADNT1 in leaves of the *Arabidopsis thaliana* wild type (Col-0), homozygous mutants ($ADNT1^{-1}/ADNT1^{-1}$) and antisense lines (line 10 and 22). Gene-specific primers were used to amplify ADNT1 (adenine nucleotide Transporter 1) from total cDNA. The reference gene, GAPDH (Glyceraldehyde 3-phosphate dehydrogenase), was used for normalization of gene transcript levels among all samples.

3.2 Phenotypes of plants with lower expression of ADNT1 transporter

Similar to the phenotype previously observed (Palmieri et al 2008), under optimal conditions for *Arabidopsis* growth, there were no visible aberrant phenotypes in the mutants during vegetative growth. After four weeks of cultivation under short-day (8 h light/16 h dark) the antisense lines and homozygous plants (*adnt1*) were transferred to dark conditions alongside WT plants. All of the homozygous mutant plants started to wilt and show signs of senescence after 7 days of darkness, whereas WT exhibited only mild signs of senescence and no visible abnormalities (Figure 2). WT plants showed clear signs of senescence only after 10 days of darkness while after 15 days of darkness transform plants were apparently dead. After 7 days plants from line 22 also showed strong signs of senescence but with a less severe phenotype than *adnt1* and line 10 plants, showing an intermediate leaf senescence phenotype between WT plants and the others two lines and thus indicating a clear correlation between the reduction in ADNT1 expression level and leaf senescence.

To further investigate this accelerated senescence in mutant plants, I measured chlorophyll content and photochemical efficiency (maximum variable fluorescence/maximum yield of fluorescence [F_v/F_m]), two parameters related to the function of chloroplasts as diagnostics of leaf senescence (Oh et al., 1996). During extended dark conditions, total chlorophyll content declined more rapidly in plants with reduced expression of ADNT1 than in WT plants (Figure 3A), and it was associated with a minor increase in the chlorophyll *a/b* ratio (Figure 3B), a typical feature of senescence-related chlorophyll breakdown in *Arabidopsis* (Pružinská et al., 2005). Accordingly, these results were associated with a more rapid decline in the photochemical efficiency of photosystem II (PSII) (F_v/F_m) in the mutants (Figure 3C).



Figure 2. Phenotypic characterization of *Arabidopsis* genotypes with reduced expression of ADNT1 under extended dark treatment. Pictures of 4-week-old, short-day-grown *Arabidopsis* plants immediately (0 d) and after further treatment for 3, 7, 10 and 15 days in darkness conditions.

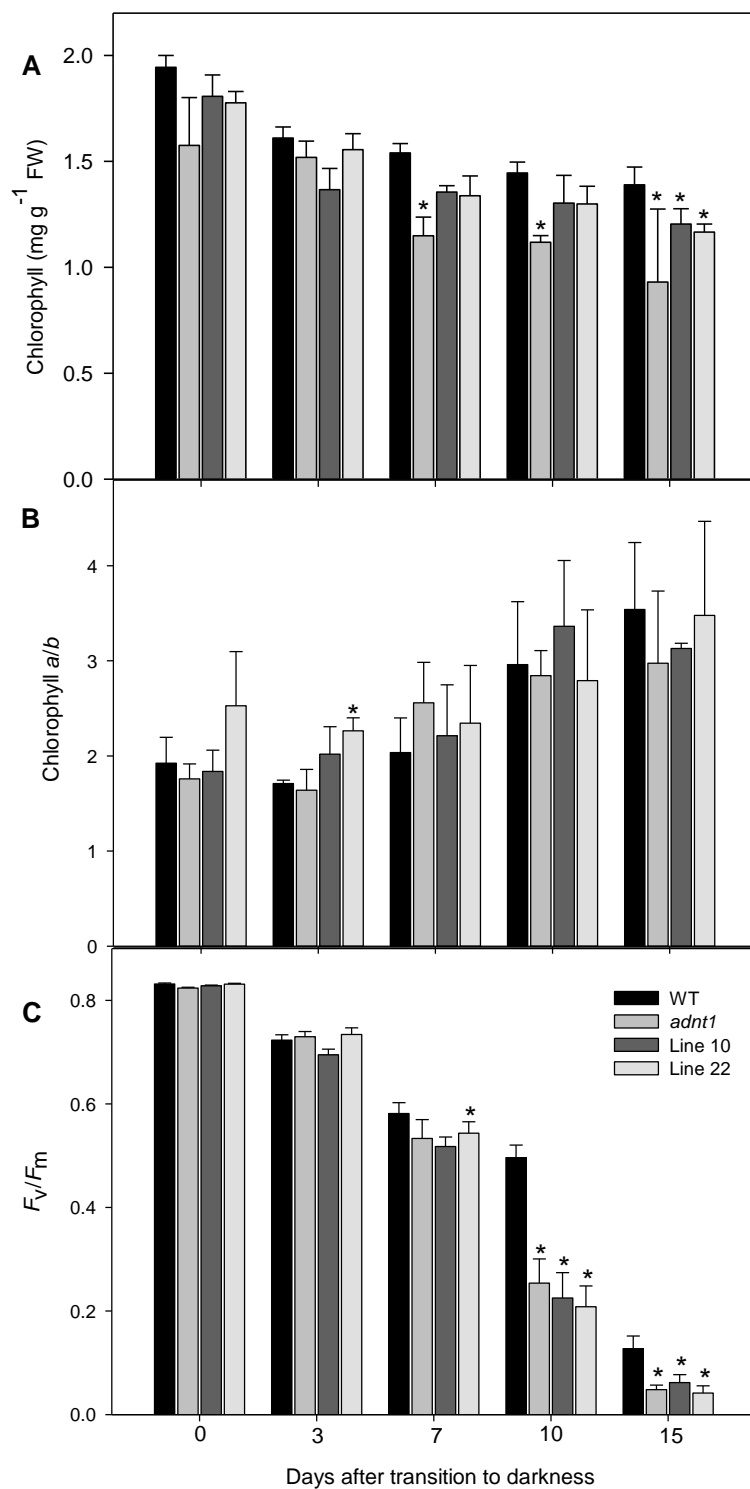


Figure 3. Phenotype of *Arabidopsis* genotypes with reduced expression of ADNT1 under extended dark treatment. Chlorophyll content (A), chlorophyll *a/b* ratio (B), and F_v/F_m (C), the maximum quantum yield of PSII electron transport, of leaves of 4-week-old, short-day-grown, *Arabidopsis* plants after further treatment for 0, 3, 7, 10, and 15 days in extended darkness. Values are means \pm standard error of five independent samplings; an asterisk indicates values that were determined by the Student's *t* test to be significantly different ($P < 0.05$) from the WT. FW, fresh weight.

For a more detailed characterization of the function of ADNT1, biochemical analyzes were performed. I first determined the levels of starch, nitrate, total amino acids, total protein, malate, fumarate and sugars (sucrose, glucose and fructose). Regarding the sugar levels, the extended darkness led to a decline in sucrose and glucose in all genotypes analyzed (Figures 4A and 4B, respectively). Surprisingly, fructose levels were not decreased like sucrose and glucose, over the dark treatment period (Figure 4C). Moreover, the levels of starch (Figure 4D) and nitrate (Figure 5C) declined during the extended darkness in a similar way for all genotypes analyzed. Interestingly, it could be noted a dramatic decline in starch level already after 3 days of darkness, with little changes thereafter. It should be noted that all genotypes used in this study showed loss of protein content (Figure 5A). Accordingly, after 15 days of continuous darkness the *adnt1* displayed significant increase in total amino acids and decrease in total protein content. The data were submitted to the Pearson correlation test that revealed a correlation ($r= -0.60$) between increase in the amino acids levels and decrease in protein content (data not shown).

Both organic acids malate (Figure 5D) and fumarate (Figure 5E) increased at the end of dark treatment. It is important to mention that malate increased significantly only in line 22 at 10 days, whereas following 15 days in darkness the levels of fumarate increased significantly in all the genotypes with higher levels being observed in *adnt1* and line 10.

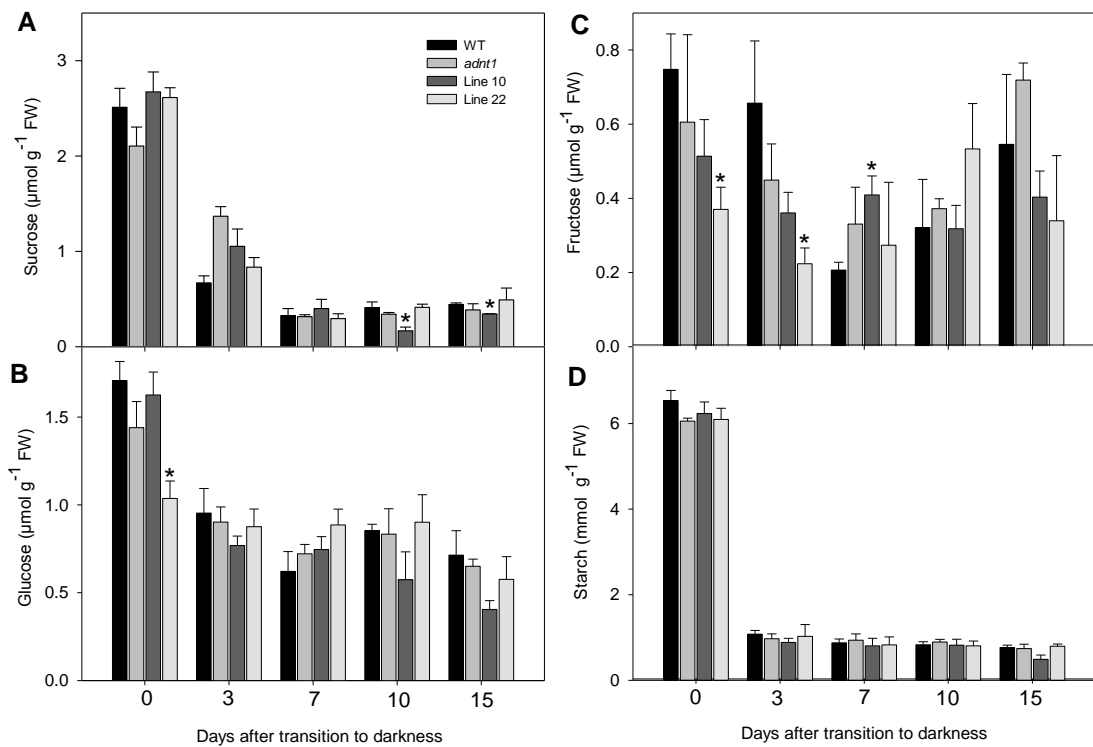


Figure 4. Changes in the main carbon related compounds in leaves of *Arabidopsis* genotypes with reduced expression of ADNT1 under extended dark treatment. Levels of sucrose (A), glucose (B), fructose (C) and starch (D) were measured. Values are means \pm standard error of five independent samplings. Asterisk indicates values that were determined by the Student's *t*-test to be significantly different ($P < 0.05$) from the WT plants. FW, fresh weight.

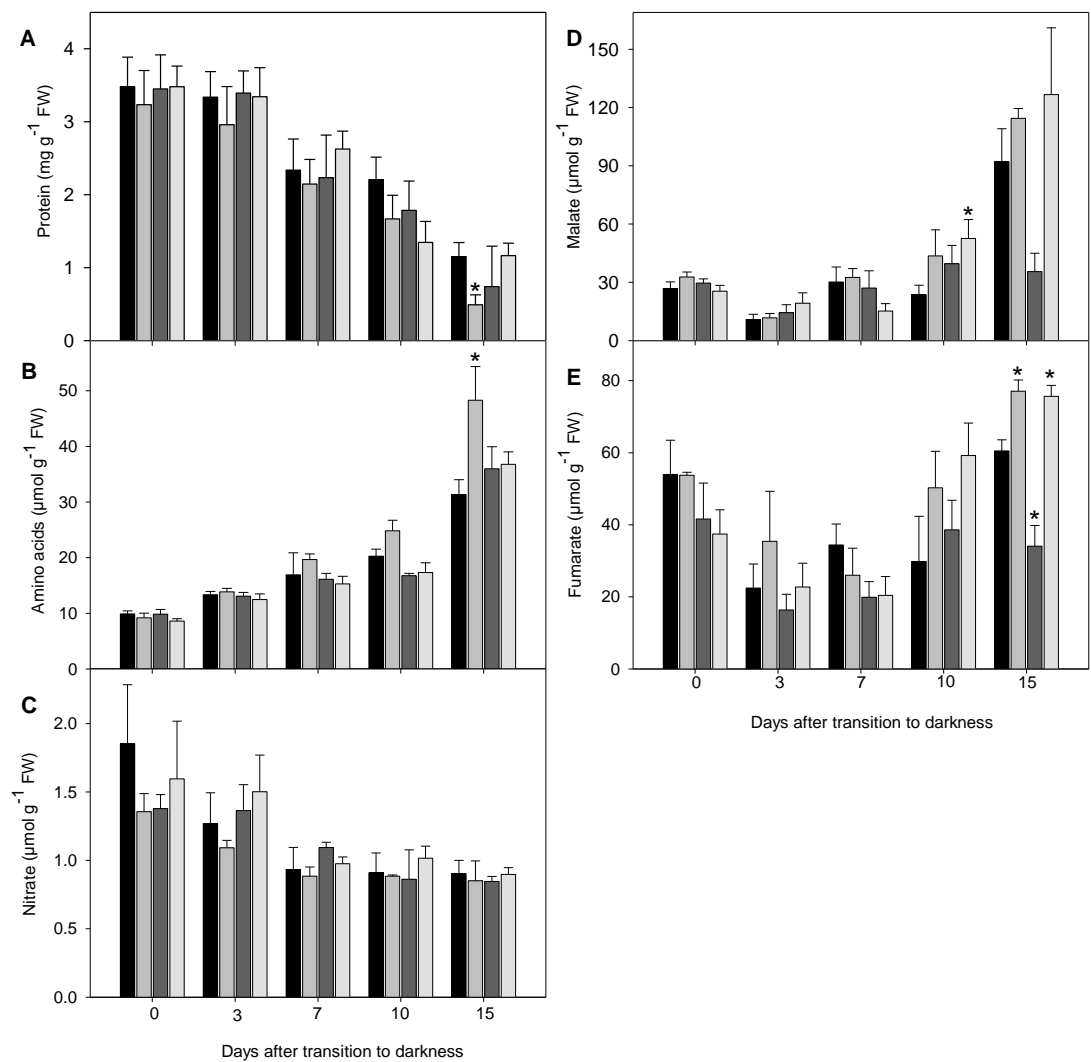


Figure 5. Changes in the main nitrogen related compounds and organic acids in leaves of *Arabidopsis* genotypes with reduced expression of ADNT1 under extended dark treatment. Levels of total protein (A), total amino acids (B), nitrate (C), malate (D), and fumarate (E) during extended dark conditions. Values are means \pm standard error of five independent samplings. Asterisk indicates values that were determined by the Student's *t*-test to be significantly different ($P < 0.05$) from WT plants. FW, fresh weight.

In order to obtain a clearer picture of the changes in the primary metabolism I next utilized an established gas chromatography-mass spectrometry (GC-MS)-based metabolic profiling method (Fernie et al., 2004; Lisec et al., 2006) to quantify the relative metabolite levels during the extended dark treatment. The extended dark treatment led to a decline in sucrose and other sugars in all genotypes analyzed (Figure 6). By contrast, the TCA cycle intermediates citrate, isocitrate and malate generally increased at the end of dark treatment (Figure 6).

It is of interest that γ -amino butyric acid (GABA) (Figure 6) and most of the free amino acids, (Figure 7) including arginine, β -Alanine, α -oleucine, lysine, methionine, phenylalanine, serine, threonine, tyrosine, tryptophan, and valine increased significantly in all genotypes during the darkness, , indicating an increased protein degradation, as previously observed (Araújo et al., 2011) (and subsequent metabolism in the case of GABA) under the experimental conditions. However, the levels of glutamate and proline declined. When taken together with the elevated levels of GABA, these data are likely indicative of an upregulation of the GABA shunt as an alternative source of mitochondrial succinate (Studart-Guimarães et al., 2007).

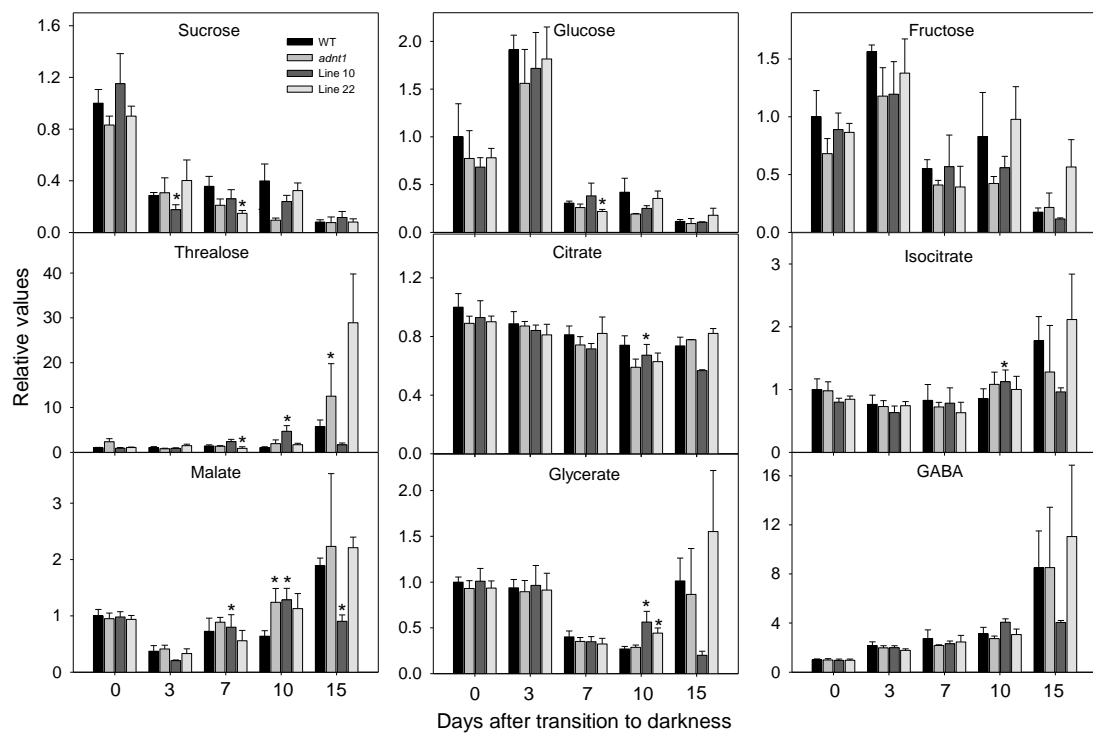


Figure 6. Relative levels of sugars and organic acids in leaves of *Arabidopsis* genotypes with reduced expression of ADNT1 under extended dark treatment. The y axis values represent the metabolite level relative to the wild type (WT). Data were normalized to the mean response calculated for the day 0 of dark-treated leaves of the WT. Values presented are X fold change \pm standard error of determinations on five independent samplings; an asterisk indicates values that were determined by the Student's *t* test to be significantly different ($P < 0.05$) from the WT.

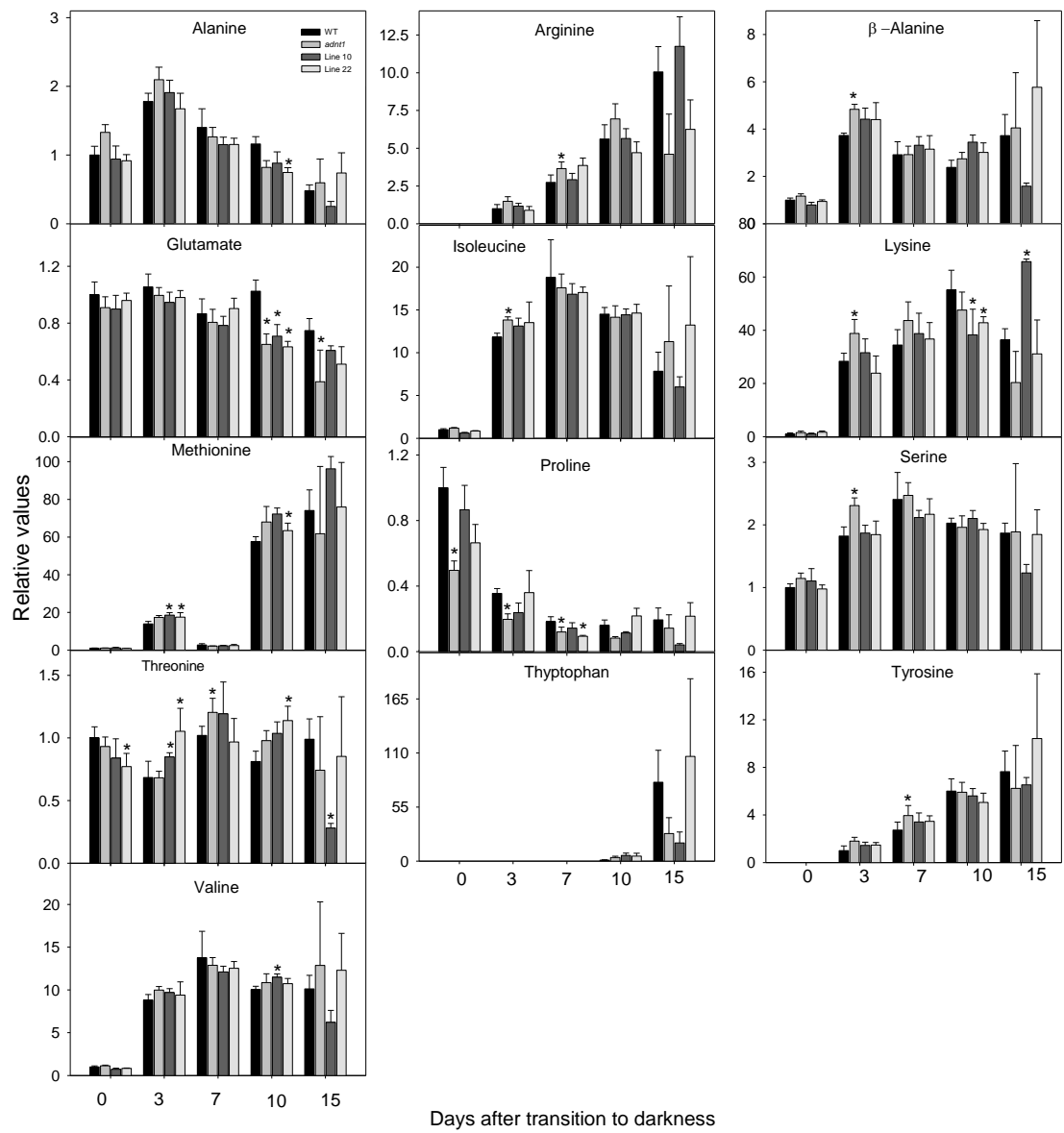


Figure 7. Relative levels of amino acids in leaves of *Arabidopsis* plants with reduced expression of ADNT1 under extended dark treatment. Levels of the indicated amino acids are presented as indicated in the Figure 6. WT, wild type.

Since ADNT1 is supposed to export ATP from the mitochondrial matrix in an exchange by AMP and, to a lesser extent, ADP, its reduced expression could also affect the redox poise in the mutants. I therefore assayed the levels of pyridine dinucleotides during extended dark conditions (Figure 8). Interestingly, whilst both NAD⁺ and NADP⁺ remained nearly constant (Figures 8B and E), NADH and NADPH levels were

significantly higher in all genotypes following the extended darkness (Figures 8A and D). As a result, a trend towards an increase in both the NADH/NAD⁺ and NADPH/NADP⁺ ratios was observed (Figures 8C and F) during dark-induced senescence. After 7 days of darkness the NADH/NAD⁺ ratio was significantly higher in the mutants than in the WT plants, whereas the NADPH/NADP⁺ ratio was significantly higher at 10 days in *adnt1* and line 10 plants.

In order to gain insight into the impact of the reduction in the expression of ADNT1 under normal growth conditions, I evaluated physiological parameters such as dark respiration (R_d) and the net CO₂ assimilation (A) in the plants. R_d was not significantly affected in the mutants (Figure 9A). Despite the fact that many perturbations in mitochondrial metabolism have been reported to result in alterations in photosynthetic metabolism (for a review see Araújo et al., 2012), the ADNT1 mutant displayed unaltered rates of relative electron transport (ETR) (Figure 9B) as well as A (Figure 9C) and stomatal conductance (g_s) (Figure 9D).

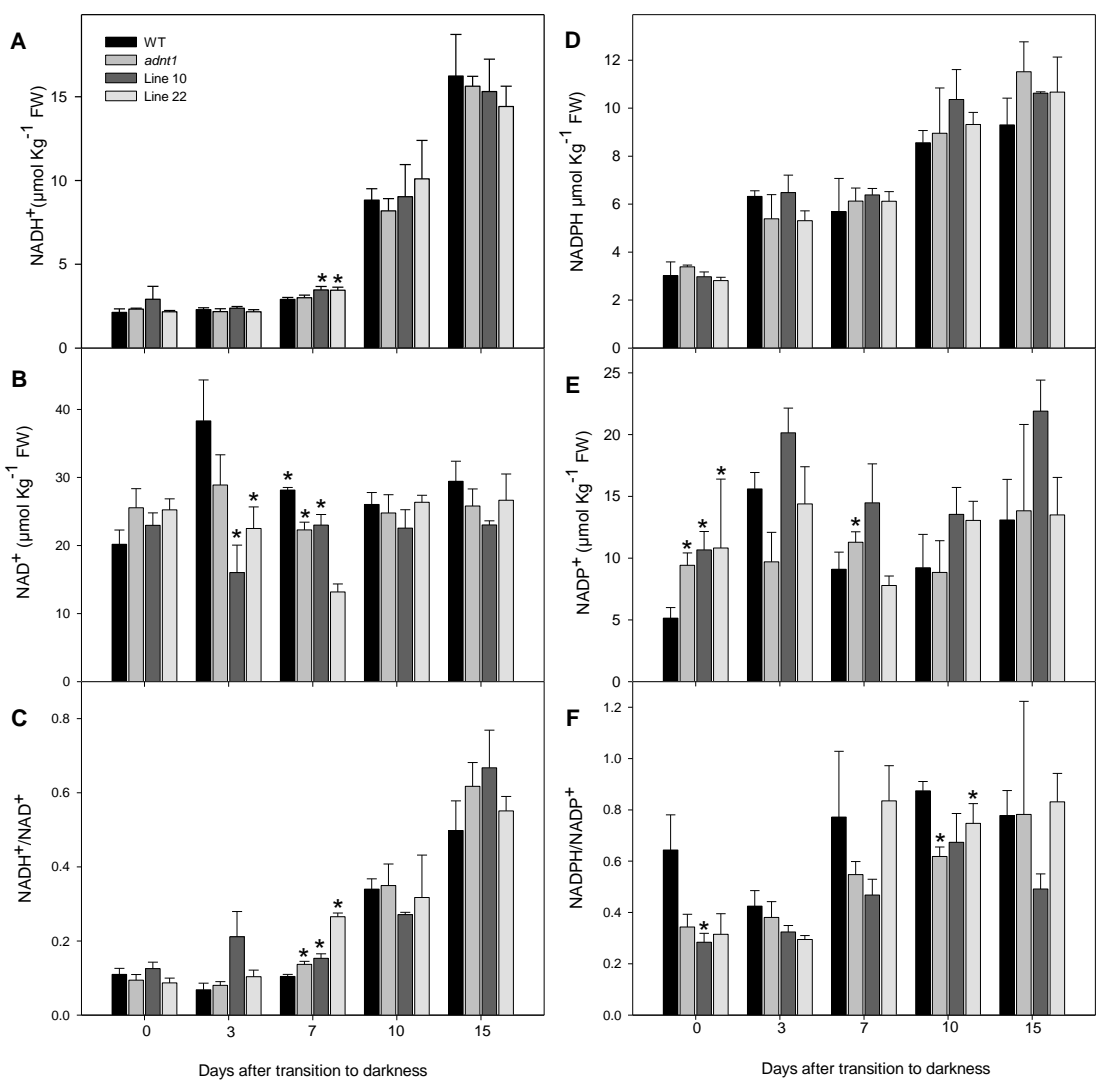


Figure 8. Pyridine nucleotide levels and ratios in leaves of *Arabidopsis* plants with reduced expression of ADNT1 under extended dark treatment. Levels of pyridine nucleotide [NADH (A), NAD⁺ (B), NADPH (D), and NADP⁺ (E)] and ratios [NADH/NAD⁺ (C) and NADPH/NADP⁺ (F)] were measured. Values are means \pm standard error of five independent samplings; an asterisk indicates values that were determined by the Student's *t* test to be significantly different ($P < 0.05$) from the WT plants. FW, fresh weight.

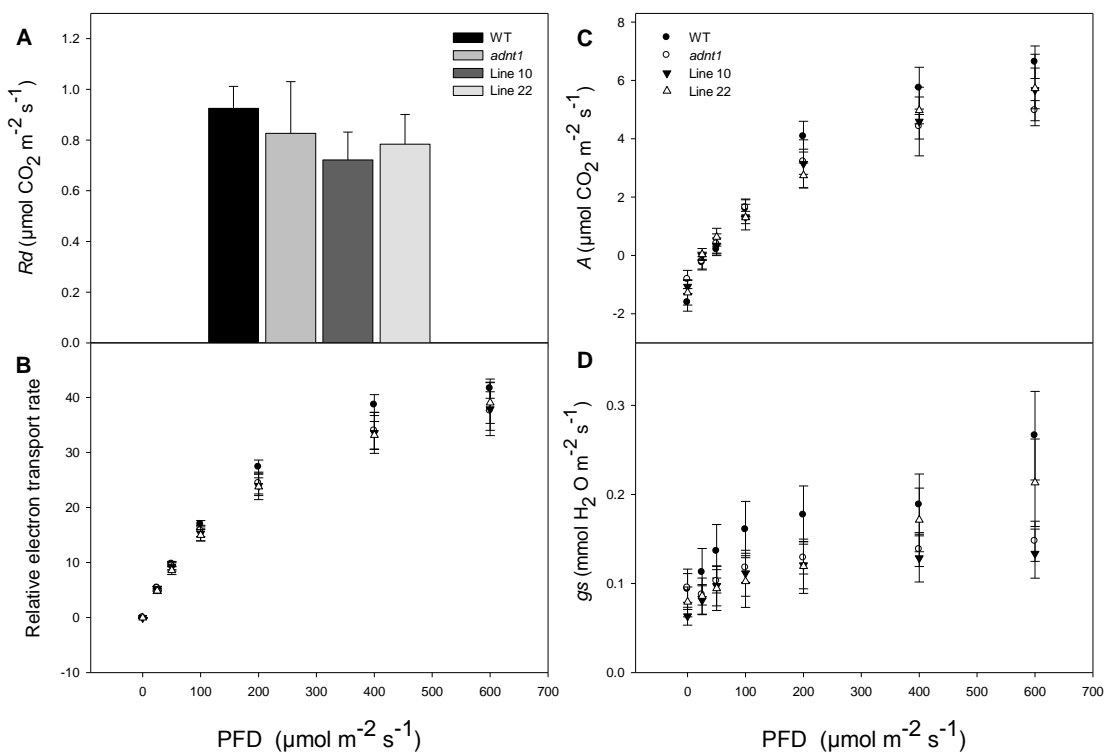


Figure 9. Effect of decreased ADNT1 expression on respiration and photosynthetic parameters in 4–5-week-old plants. (A) Dark respiration (R_d). Values are presented as mean \pm standard error of six determinations per line. (B) *In vivo* chlorophyll fluorescence measured as an indicator of the electron transport rate by use of a fluorometer at photon flux densities (PFDs) ranging from 25 to 600 $\mu\text{mol m}^{-2} \text{sec}^{-1}$. (C) Assimilation rate (A) and (D) stomatal conductance (g_s) as a function of light intensity.

3.3 Natural senescence phenotype in leaves of *Arabidopsis* plants with reduced expression of ADNT1

Although ADNT1 is apparently not essential under standard growth conditions (Palmieri et al., 2008), it may become more relevant under specific environmental conditions or stresses. Therefore I tested two different growth conditions, including long-day (16 h light/8 h dark) and short-day (8 h light/16 h dark). In both conditions tested, the mutant plants exhibited symptoms of early senescence in comparison to the WT plants (Figure 10). This suggests an important role for the ADNT1 not only during

the severe stress condition, as observed during extended darkness, but also under more physiologically experienced by most plants at some stage during their life cycle.

Interestingly it was previously observed that ADNT1 promoter-GUS fusion expression upon wounding or senescence, culminated in high GUS activity predominantly on leaves edges (Palmieri et al., 2008), coinciding with the anticipated senescence pattern displayed by ADNT1 mutants (Figure 10)

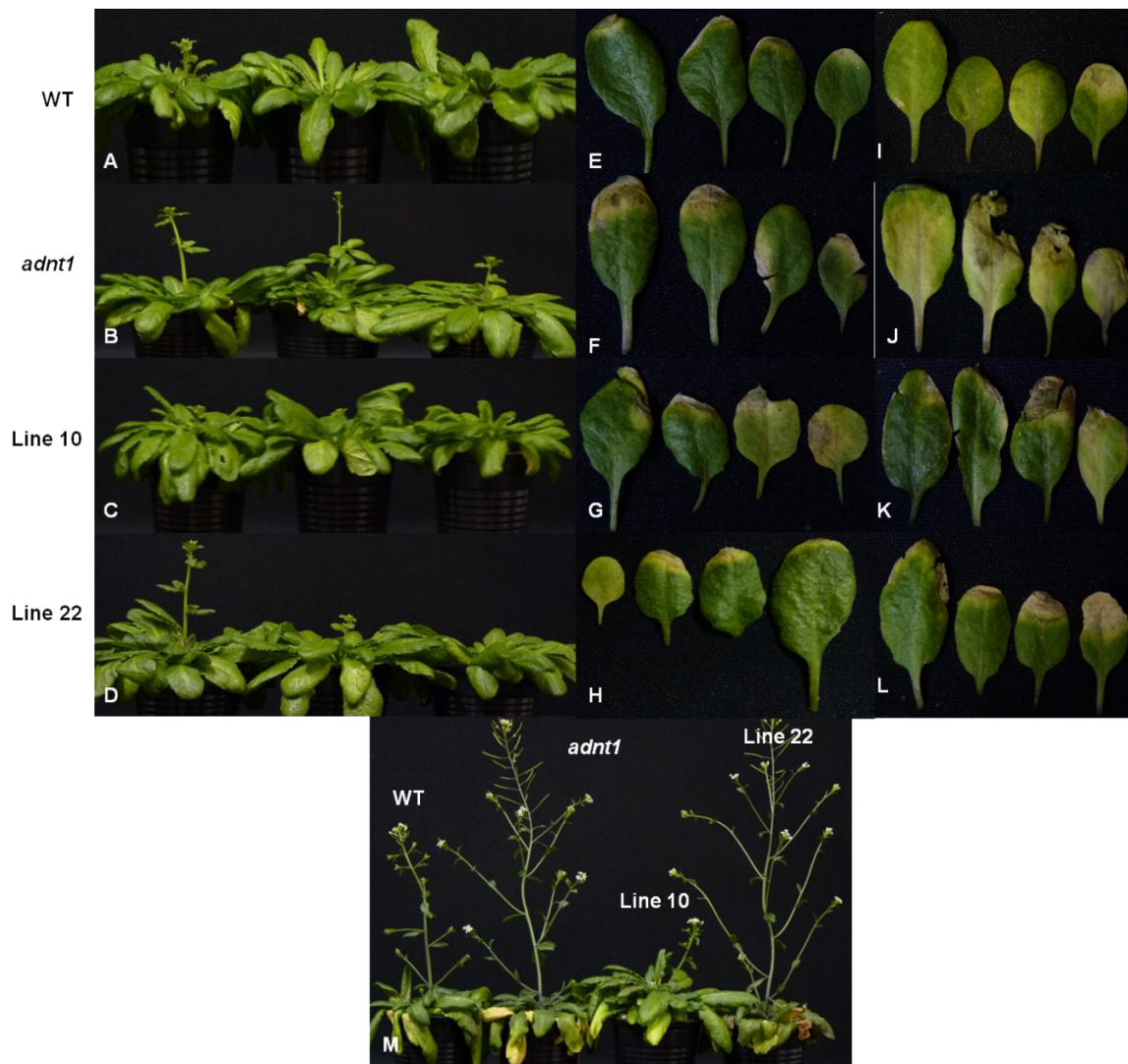


Figure 10. Natural senescence phenotypes in leaves of *Arabidopsis* genotypes with reduced expression of ADNT1. The plants were grown under a short day light regime for 4 weeks and then transferred to specific condition: (A, B, C, D, E, F, G and H) short day (8h light/16h dark) conditions and (E, I, J, K, L and M) long day conditions (16h light/8h dark). In all conditions tested the mutant plants exhibited symptoms of early senescence when compared to WT plants.

4 DISCUSSION

4.1 Physiological Relevance of ADNT1 in the Metabolism of *Arabidopsis*

Since the deficiency of ADNT1 did not seem to greatly alter photosynthetic metabolism and growth (Figures), ADNT1 is apparently not essential under our standard growth conditions (long days) as previously observed (Palmieri et al., 2008). However, the data presented here suggests that it may become more relevant under specific environmental conditions or stresses. Although expression studies revealed that ADNT1 is expressed across a broad range of tissue types, analysis of the expression of GUS suggested that ADNT1 expression is much stronger in root tips and senescing tissues (Palmieri et al., 2008). Moreover, isolation and characterization of a T-DNA insertional knockout mutant of ADNT1, alongside complementation and antisense approaches, demonstrated that deficiency of this transporter resulted in reduced root growth and respiration (Palmieri et al., 2008). Therefore, considering the high expression in senescing tissues, I decided investigate the role of ADNT1 during the process of dark-induced senescence, which mimics situations of carbon starvation. Under these conditions, plants with low expression of ADNT1 displayed a similar, yet milder, early onset of senescence (Figures 2 and 3). Interestingly, the mutant plants also exhibited symptoms of early senescence in comparison to the WT plants even under non-stressful conditions (Figure 10). These data thus demonstrate that ADNT1 is not functionally redundant to the previously characterized ADP/ATP carriers, especially during carbon starvation and reinforce the potential function for ADNT1 in the provision of the energy required to support growth in heterotrophic plant tissues, like root and senescing tissues. During the dark-induced senescence process, there is an increased catabolic activity. Chlorophyll and macromolecules such as proteins, sugars, starch, lipids and nucleic acids are degraded and breakdown products can provide electrons to the electron transport chain

in the mitochondria for maintaining the rate of respiration. In the case of *Arabidopsis thaliana* mutants deficient in the expression of ADNT1 transporter, the extended dark treatment led in general to a more rapidly decline than in the wild type in the chlorophyll content (figure 3A) and in the levels of sucrose (figure 4A) and protein (figure 5A). On the other hand, the levels of total amino acids (Figure 5B), most of the free amino acids (Figure 7) and of the TCA cycle intermediates malate (Figure 5D), fumarate (Figure 5E) and isocitrate (Figure 6) generally increased significantly in the mutants at the end of dark treatment. The ratios NADH/NAD⁺ and NADPH/NADP⁺ also showed tendency to increase in mutants in comparison to the wild type with progression of the darkness (Figure 8). These data thus demonstrate that the reduction in the expression of ADNT1 is associated to a higher consumption of respiratory substrates during conditions of dark-induced senescence. Furthermore, the accumulation of TCA cycle intermediates is likely indicative of the reduction in the activity of dehydrogenases of the TCA cycle. Upon the decrease in the expression of ADNT1, there is likely a lower export of ATP to the cytosol, thereby leading to a decrease of ADP in the mitochondrial matrix, which in turn leads to an increase in the inner membrane potentials of mitochondria. A high mitochondrial membrane potential restricts electron flow and thus leads to a lower oxidation of NADH. Therewith, there is an accumulation of NADH in the cytosol bringing as consequence the accumulation of TCA cycle intermediates commented previously.

A constant supply of the substrate for oxidative phosphorylation (ADP) via adenylate kinase equilibrium maintains operative mitochondria and prevents side-effects due to accumulation of NADH and other reduced products of metabolism (Igamberdiev & Kleczkowski, 2006). The side-effects could include formation of the potentially harmful superoxide and other reactive oxygen species (Igamberdiev & Kleczkowski,

2006). In addition to its potential role in oxidative phosphorylation, the availability of ADP in the intermembrane space is of high importance for the homeostatic maintenance of respiration, and a good supply of this substrate should serve to prevent side effects due to the accumulation of NADH and other reduced products of metabolism. It has long been evident that other proteins in the inner mitochondrial membrane, in addition to complex I, oxidize both internal and external NADH and NADPH. Additional components like internal and external NAD(P)H dehydrogenases, alternative oxidase (AOX), as well as the membrane-potential-dissipating uncoupling proteins (UCPs) constitute non-phosphorylating by-passes in that they don't contribute to the generation of the inner-membrane proton gradient. These by-passes allow electron transport to continue even when membrane potential ($\Delta\psi$) is high, thereby uncoupling electron transport from ATP synthesis (Fernie et al. 2004; Rasmusson et al., 2004). When taken together with our work here, these studies are likely indicative of a possible increase in the activity of alternative respiratory enzymes, AOX and UCP. That would explain why there was only mild changes in the levels of NADH and TCA cycle intermediates.

Unlike other ADP/ATP carriers, ADNT1 is the unique that mediates an antiport of ATP, AMP, and, to a lesser extent, ADP and the corresponding deoxyadenine nucleotides and is not inhibited by bongkrekate and carboxyatractyloside (Palmieri et al., 2008). It is known that in heterotrophic plant tissues, such as roots, AMP is the predominant nucleotide in the cytosol. Additionally, cytosolic AMP increases markedly in plant tissues during emergence from dormancy and during stresses such as anoxia and is primarily converted to ATP during recovery from these stresses (Saglio et al., 1980; Standard et al., 1983; Raymond et al., 1985). Exported ATP from the matrix and cytosolic AMP can be converted in the intermembrane space by the adenylate kinase into two molecules of ADP, which re-enter the mitochondrial matrix via the ADP/ATP

carrier to support ATP synthesis (Roberts et al., 1997). Given these transport features, it is likely that the physiological function of ADNT1 is the import of cytosolic AMP in counter-exchange with mitochondrial ATP (Palmieri et al., 2008). That said, the fact that the lower expression of ADNT1 results in a restricted rate of root respiration, in a reduced root growth (Palmieri et al., 2008) and in the early onset of dark-induced senescence is consistent with the proposed role of ADNT1 in plants in the provision of the energy required to support growth in heterotrophic plant tissues.

In summary, this work suggests that ADNT1 transporter has a physiological relevance not only in heterotrophic tissues but also in autotrophic tissues under carbon starvations conditions. Additionally, our results suggest that ADNT1 transport plays a role in processes related to natural senescence events.

5 REFERENCES

- Araújo WL, Nunes-Nesi A, Osorio S, Usadel B, Fuentes D, Nagy R, Balbo I, Lehmann M, Studart-Witkowski C, Tohge T, Metinoia E, Jordana X, DaMatta FM, Fernie AR** (2011) Antisense inhibition of the ironsulphur subunit of succinate dehydrogenase enhances photosynthesis and growth in tomato via an organic acid-mediated effect on stomatal aperture. *Plant Cell* **23**: 600–627.
- Araújo WL, Nunes-Nesi A, Nikoloski Z, Sweetlove LJ, Fernie AR** (2012) Metabolic control and regulation of the tricarboxylic acid cycle in photosynthetic and heterotrophic plant tissues. *Plant Cell Environ* **35**: 1–21
- Arvidsson S, Kwasniewski M, Riano-Pachon DM, Mueller-Roeber B** (2008) QuantPrime - a flexible tool for reliable high-throughput primer design for quantitative PCR. *BMC Bioinformatics* **9**: 465
- Bauwe H, Hagemann M, Fernie A.R.** (2010) Photorespiration: players, partners and origin. *Trends Plant Sci* **15**: 330–336
- Braütigam A, Weber, APM** (2011) Do metabolite transport processes limit photosynthesis? *Plant Physiol* **155**: 43–48
- Buchanan BB, Grussem W, Russel LJ** (2000) *Biochemistry and Molecular Biology of Plants*. American Society of Plant Physiologists, Rockville, Maryland
- Castegna A, Scarcia P, Agrimi G, Palmieri L, Rottensteiner H, Spera I, Germinario L, Palmieri F** (2010) Identification and functional characterization of a novel mitochondrial carrier for citrate and oxoglutarate in *Saccharomyces cerevisiae*. *J. Biol.Chem.* **285**: 17359–17370
- Clough SJ, Bent AF** (1998) Floral dip: a simplified method for *Agrobacterium*-mediated transformation of *Arabidopsis thaliana*. *Plant J* **16**: 735–743
- Eisenhut M, Georg J, Klähn S, Sakurai I, Mustila H, Zhang P, Hess WR** (2012) The antisense RNA as1_flv4 in the *Cyanobacterium Synechocystis* sp. PCC 6803 prevents premature expression of the flv4-2 operon upon shift in inorganic carbon supply. *J. Biol. Chem.* **287**: 33153–33162
- Fernie AR, Roscher A, Ratcliffe RG, Kruger NJ** (2001) Fructose 2,6-bisphosphate activates pyrophosphate: fructose-6-phosphate 1-phosphotransferase and increases triose phosphate to hexose phosphate cycling in heterotrophic cells *Planta* **212**: 250–263
- Fernie AR, Carrari F, Sweetlove LJ** (2004) Respiratory metabolism: glycolysis, the TCA cycle and mitochondrial electron transport. *Curr Opin. Plant Biol* **7**: 254–261
- Fernie AR, Aharoni A, Willmitzer L, Stitt M, Tohge T, Kopka J, Carroll AJ, Saito K, Fraser PD, DeLuca V** (2011). Recommendations for reporting metabolite data. *Plant Cell* **23**: 2477–2482.

Foyer CH, Noctor G, Hodges M (2011) Respiration and nitrogen assimilation: targeting mitochondria-associated metabolism as a means to enhance nitrogen use efficiency. *J Exp Bot* **62**: 1467–1482

Fritz C, Palacios-Rojas N, Feil R, Stitt M (2006) Regulation of secondary metabolism by the carbon-nitrogen status in tobacco: nitrate inhibits large sectors of phenylpropanoid metabolism. *Plant J* **46**: 533-548

Fuentes D, Meneses M, Nunes-Nesi A, Araújo WL, Tapia R, Gómez I, Holuigue L, Gutiérrez RA, Fernie AR, Jordana X (2011) A Deficiency in the Flavoprotein of *Arabidopsis* Mitochondrial Complex II Results in Elevated Photosynthesis and Better Growth in Nitrogen-Limiting Conditions. *Plant Physiol* **157**: 1114-1127

Geigenberger P, Rieve D, Fernie AR (2010) The central regulation of plant physiology by adenylates. *Trends Plant Sci* **15**: 1360-1385

Gibon Y, Blaesing OE, Hannemann J, Carillo P, Hoehne M, Hendriks JHM, Palacios N, Cross J, Selbig J, Stitt M (2004) A robot-based platform to measure multiple enzyme activities in *Arabidopsis* using a set of cycling assays: Comparison of changes of enzyme activities and transcript levels during diurnal cycles and in prolonged darkness. *Plant Cell* **16**: 3304-3325

Haferkamp I, Hackstein JHP, Voncken FGJ, Schmit G, Tjaden J (2002) Functional integration of mitochondrial and hydrogenosomal ADP/ATP carriers in the *Escherichia coli* membrane reveals different biochemical characteristics for plants, mammals and anaerobic chytrids. *Eur J Biochem* **269**: 3172-3181

Haferkamp I, Fernie AR, Neuhaus HE (2011) Adenine nucleotide transport in plants: much more than a mitochondrial issue *Trends Plant Sci* **16**: 507-515

Haferkamp I & Schmitz - Esser (2012) The plant mitochondrial carrier family: functional and evolutionary aspects. *Front. Plant Sci.* **3**: 2

Hanning I & Heldt HW (1993) On the function of mitochondrial metabolism during photosynthesis in spinach (*Spinacia oleracea*) Leaves. *Plant Physiol* **103**: 1147-1 154

Igamberdiev AU & Kleczkowski LA (2006) Equilibration of adenylates in the mitochondrial intermembrane space maintains respiration and regulates cytosolic metabolism. *J Exp Bot* **57**: 2133-2141

Jeter CR, Tang W, Henaff E, Butterfield T, Roux SJ (2004) Evidence of a novel cell signaling role for extracellular adenosine triphosphates and diphosphates in *Arabidopsis*. *Plant Cell* **16**: 2652-2664

Klingenberg M (2008) The ADP and ATP transport in mitochondria and its carrier. *Biochim Biophys Acta* **1778**: 1978-2021

Leroch M, Neuhaus HE, Kirchberger S, Zimmermann S, Melzer M, Gerhold J, Tjaden J (2008) Identification of a novel adenine Nucleotide transporter in the endoplasmic reticulum of *Arabidopsis*. *Plant Cell* **20**: 438-451

Lima ALS, DaMatta FM, Pinheiro HA, Totola MR, Loureiro ME (2002) Photochemical responses and oxidative stress in two clones of *Coffea canephora* under water deficit conditions. *Environ Exp Bot* **47**: 239-247

Linka N, Theodoulou FL, Haslam RP, Linka M, Napier JA, Neuhaus HE, Weber APM (2008) Peroxisomal ATP import is essential for seedling development in *Arabidopsis thaliana*. *Plant Cell*, **20**: 3241-3257

Linka, N & Weber, APM (2010) Intracellular metabolite transporters in plants. *Mol Plant* **3**: 21-53

Lisec J, Schauer N, Kopka J, Willmitzer L, Fernie AR (2006) Gas chromatography mass spectrometry-based metabolite profiling in plants. *Nat Protoc* **1**: 387-396

Lunn JE (2007) Compartmentation in plant metabolism. *J Exp Bot* **58**: 35–47

Macherel D, Benamar A, Avelange-Macherel M, Tolleter D (2007) Function and stress tolerance of seed mitochondria. *Physiol Plant* **129**: 233–241.

Mäser P, Thomine S, Schroeder JI, Ward JM, Hirschi K, Sze H, Talke IN, Amtmann A, Maathuis FJM, Sanders D, Harper JF, Tchieu J, Gribskov M, Persans MW, Salt DE, Kim SA, Guerinot ML (2001) Phylogenetic relationships within cation transporter families of *Arabidopsis*. *Plant Physiol* **126**: 1646-1667

Millar AH, Heazlewood (2003) Genomic and proteomic analysis of mitochondrial carrier proteins in *Arabidopsis*. *Plant Physiol* **131**: 443-453

Millar AH, Whelan J, Soole KL, Day DA (2011) Organization and regulation of mitochondrial respiration in plants. *Annu Rev Plant Biol* **62**: 79-104

Möhlmann T, TjadennJ, Schwöppe C, Winkler HH, Kampfenkel K, Neuhaus HE (1998) Occurrence of two plastidic ATP/ADP transporters in *Arabidopsis thaliana* L Molecular characterisation and comparative structural analysis of similar ATP/ADP translocators from plastids and *Rickettsia prowazekii*. *Eur J Biochem* **252**: 353-359

Nunes-Nesi A, Carrari F, Lytovchenko A, Smith AMO, Loureiro ME, Ratcliffe RG, Fisahn J, Sweetlove LJ, Fernie AR (2005) Enhanced photosynthetic performance and growth as a consequence of decreasing mitochondrial malate dehydrogenase activity in transgenic tomato plants. *Plant Physiol*. **137**: 611-622.

Nunes-Nesi A, Carrari F, Gibon Y, Sulpice R, Lytovchenko A, Fisahn J, Graham J, Ratcliffe RG, Sweetlove LJ, Fernie AR (2007) Deficiency of mitochondrial fumarase activity in tomato plants impairs photosynthesis via an effect on stomatal function. *The Plant J* **50**: 1093–1106

Nury H, Dahout - Gonzalez C, Trézéguit V, Lauquin GJM, Brandolin G, Pebay - Peyroula E (2006) Relations Between Structure and Function of the Mitochondrial ADP/ATP Carrier. *Annu. Rev. Biochem.* **75**: 713-741

Oh SA, Lee SY, Chung IK, Lee CH, Nam HG (1996) A senescence-associated gene of *Arabidopsis thaliana* is distinctively regulated during natural and artificially induced leaf senescence. *Plant Mol Biol* **30**: 739-754

Palmieri F, Pierri CL, Grassi A, Nunes-Nesi A, Fernie AR (2011) Evolution, structure and function of mitochondrial carriers: a review with new insights. *Plant J* **66**: 161-181

Palmieri F, Rieder B, Ventrella A, Blanco E, Do PT, Nunes-Nesi A, Trauth AU, Fiermonte G, Tjaden J, Agrimi G, Kirchberger S, Paradies E, Fernie AR, Neuhaus HE (2009) Molecular identification and functional characterization of *Arabidopsis thaliana* mitochondrial and chloroplastic NAD⁺carrier proteins. *J Biol Chem* **284**: 31249-31259

Palmieri L, Santoro A, Carrari F, Blanco E, Nunes-Nesi A, Arrigone R, Genchi F, Fernie AR, Palmieri F (2008) Identification and characterization of ADNT1, a novel mitochondrial adenine nucleotide transporter from *Arabidopsis*. *Plant Physiol* **148**: 1797-1808

Picault N, Palmieri L, Pisano I, Hodges M, Palmieri F (2002) Identification of a novel transporter for dicarboxylates and tricarboxylates in plant mitochondria: bacterial expression, reconstitution, functional characterization, and tissue distribution. *J Biol Chem* **277**: 24204-24211

Picaut N, Hodges M, Palmieri L, Palmieri F (2004) The growing family of mitochondrial carriers in *Arabidopsis*. *Trends Plant Sci* **9**: 138-146

Poirier Y & Bucher M (2002) Phosphate transport and homeostasis in *Arabidopsis*. The *Arabidopsis* Book. DOI: 10.1199/tab.0024

Porra RJ, Thompson WA, Kriedemann PE (1989) Determination of accurate extinction coefficients and simultaneous equations for assaying chlorophylls a and b extracted with four different solvents: Verification of the concentration of chlorophyll standards by atomic absorption spectroscopy. *Biochim Biophys Acta* **975**: 384-394.

Pružinská A, Tanner G, Aubry S, Anders I, Moser S, Müller T, Onganía K-H, Kräutler B, Youn J-Y, Liljegren SJ, Hörtensteiner S (2005) Chlorophyll breakdown in senescent *Arabidopsis* leaves: Characterization of chlorophyll catabolic enzymes involved in the degreening reaction. *Plant Physiol* **139**: 52-63.

Rasmusson AG, Soole KL, Elthon TE (2004). Alternative NAD(P)H dehydrogenases of plant mitochondria. *Annu. Rev. Plant Biol.* **55**: 23-39

Raymond P, Alani A, Pradet A (1985) ATP production by respiration and fermentation, and energy charge during aerobiosis and anaerobiosis in 12 fatty and starchy germinating seeds. *Plant Physiol* **79**: 879-884

Reinhold, T Alawady A, Grimm B, Beran KC, Jahns P, Conrath U, Bauer J, Reiser J, Melzer M, Jeblick W, Neuhaus HE (2007) Limitation of nocturnal import of ATP into *Arabidopsis* chloroplasts leads to photooxidative damage. *Plant J* **50**: 293-304

Reiser J, Linka N, Lemke L, Jeblick W, Neuhaus HE (2004) Molecular Physiological Analysis of the Two Plastidic ATP/ADP Transporters from *Arabidopsis*. *Plant Physiol* **136**: 3524-3536

Rieder B, Neuhaus HE (2011) Identification of an *Arabidopsis* Plasma Membrane-Located ATP Transporter Important for Anther Development. *Plant Cell* **23**: 1932–1944

Roberts JKM, Aubert S, Gout E, Bligny R, Douce R (1997) Cooperation and Competition between adenylate Kinase, nucleoside diphosphokinase, electron transport, and ATP synthase in plant mitochondria studied by 31 P-nuclear magnetic resonance. *Plant Physiol* **113**: 191-199

Roessner U, Luedemann A, Brust D, Fiehn O, Linke T, Willmitzer L, Fernie AR (2001) Metabolic profiling allows comprehensive phenotyping of genetically or environmentally modified plant systems. *Plant Cell* **13**: 11-29

Rosso MG, Li Y, Strizhov N, Reiss B, Dekker K, Weisshaar B (2003) An *Arabidopsis thaliana* T-DNA mutagenized population (GABI-Kat) for flanking sequence tag-based reverse genetics. *Plant Mol Biol* **53**: 247–259

Saglio PH, Raymond P, Pradet A (1980) Metabolic activity and energy charge of excised maize root tips under anoxia control by soluble sugars. *Plant Physiol* **66**: 1053-1057

Saraste, M & Walker J (1982) Internal sequence repeats and the path of polypeptide in mitochondrial ADP/ATP translocase. *FEBS Lett* **144**: 250–254.

Schippers JHM, Nunes-Nesi A, Apetrei R, Hille J, Fernie AR, Dijkwel PP (2008) The *Arabidopsis* onset of leaf death5 mutation of quinolinate synthase affects nicotinamide adenine dinucleotide biosynthesis and causes early ageing. *Plant Cell* **20**: 2909-2925

Standard SA, Perret D, Bray CM (1983) Nucleotide levels and loss of vigor and viability in germinating wheat embryos. *J Exp Bot* **34**: 1047-1054

Studart-Guimarães C, Fait A, Nunes-Nesi A, Carrari F, Usadel B, Fernie AR (2007). Reduced expression of the succinylcoenzyme A ligase can be compensated for by up-regulation of the gamma-aminobutyrate shunt in illuminated tomato leaves. *Plant Physiol.* **145**: 626–639.

Sweetlove LJ, Fait A, Nunes-Nesi A, Williams T, Fernie AR (2007) The mitochondrion: an integration point of cellular metabolism and signalling. *Crit Rev Plant Sci* **26**: 17–43

Swidzinski JA, Sweetlove LJ, Leaver CJ (2002) A custom microarray analysis of gene expression during programmed cell death in *Arabidopsis thaliana*. *Plant J* **30**: 431-446

Taylor NL, Howell KA, Heazlewood JL, Tan TYW, Narsai R, Huang S, Whelan J, Millar AH (2010) Analysis of the rice mitochondrial carrier family reveals anaerobic accumulation of a basic amino acid carrier involved in arginine metabolism during seed germination. *Plant Physiol* 154: 691-704

Tegeder M & Weber APM (2006). Metabolite transporters in the control of plant primary metabolism. In *Control of Primary Metabolism in Plants*, Plaxton, W.C., McManus, M.T., eds (Oxford, UK: Blackwell Publishing Ltd), 85–120.

Weber APM & Linka N (2011) Connecting the plastid: transporters of the plastid envelope and their role in linking plastidial with cytosolic metabolism. *Annu. Rev. Plant Biol.* **62**:53–77

Weber APM & Bräutigam A (2012) The role of membrane transport in metabolic engineering of plant primary metabolism. *Curr Opin Biotechnol* **24**: 1-7